Marine and Petroleum Geology 162 (2024) 106752

Contents lists available at ScienceDirect

Marine and Petroleum Geology

journal homepage: www.elsevier.com/locate/marpetgeo

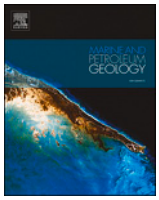

A Paleogene mixed carbonate-siliciclastic system in the western Tethys: spectral gamma-ray as a tool for the reconstruction of paleoclimate and transgressive-regressive cycles

Victor M. Giraldo-Gómez [a], Michele Piazza [a], Luca Arena [a], Andrea Baucon [a], Antonella Gandolfi [a], Cesare A. Papazzoni [b], Johannes Pignatti [c], Antonino Briguglio [a,*]

[a] Dipartimento di Scienze della Terra, dell'Ambiente e della Vita, Università degli Studi di Genova, Corso Europa 26, I-16132 Genova, Italy
[b] Dipartimento di Scienze Chimiche e Geologiche, Università di Modena e Reggio Emilia, Via Campi 103, I-41125 Modena, Italy
[c] Dipartimento di Scienze della Terra, Università degli Studi di Roma "La Sapienza", Piazzale Aldo Moro 5, I-00185, Roma, Italy

ARTICLE INFO

Keywords:
Spectral gamma-ray
Stacking patterns
Transgression
Drowning ramp
Paleoclimate
Paleogene

ABSTRACT

The mixed carbonate-siliciclastic ramps of the Dauphinois-Provençal domain in northwest Italy are characterized by a common development process during the Paleogene. Spectral gamma-ray (SGR) analysis indicates the concentration of potassium (K), uranium (U), and thorium (Th) in the total gamma-ray signal, permitting the identification of subtle stratigraphic compositional trends, sedimentary minerals, paleoclimatic conditions, and the individualization of lithofacies characters through the stacking pattern cycles. This study integrates known lithological and fossil content analysis of the section with new independent data from the spectral gamma-ray (SGR) to explore the paleoclimate and stacking patterns for defining large-scale depositional cycles along a Paleogene succession in the southwestern Alps.

The differences between the outcropping Microcodium Formation and the Capo Mortola Calcarenite Formation are indicated by the SGR, conventionally shown on a linear scale as American Petroleum Institute (API) units, i.e., Th/U, and Th/K ratios. Our data indicate lithofacies associated with normal marine to continental conditions and the presence of abundant smectite, rather than kaolinite, suggesting that the prevailing climate was characterized by prolonged dry periods. Furthermore, the SGR (API) reconstruction of the overall short cycles reflects a progradational and/or retrogradational stacking geometry that accumulated throughout the whole succession. However, the use of the derivative trend analysis (DTA) of the SGR indicates the establishment of long cycles in both formations. The short cycles observed in the Capo Mortola Calcarenite Formation are of particular importance because they characterize the marine transgression of the middle-upper Eocene, transgressive upon the Upper Cretaceous beds, and permit pinpointing the onset of the drowning ramp, which can be correlated regionally with sections spanning from the French-Italian Maritime Alps to the France-Switzerland border.

1. Introduction

Mixed carbonate-siliciclastic shallow marine systems have been studied through geologic time, displaying alternation at different scales (Mount, 1984; Longhitano et al., 2010; Zecchin and Caffau, 2011; Chiarella et al., 2017). The mixing between carbonate and siliciclastic sediments originates from different processes within the basin, where the combination of siliciclastic and carbonate grains as well as the alternation of laminas and strata sets play a role in their configuration controlled by temporal and/or spatial factors (Mount, 1984; Chiarella et al., 2017). Therefore, mixing between the two heterolithic components may occur at different proportions and scales according to different depositional processes, relative sea-level changes, and/or climatic variations, providing more sensitive records and a more complex sedimentation pattern than in pure siliciclastic or carbonate systems (Chiarella et al., 2017). For these reasons, mixed sedimentary successions are a great source of geological information, as they may provide sufficient data to completely reconstruct the paleogeographic and

* Corresponding author.
E-mail address: antonino.briguglio@unige.it (A. Briguglio).

https://doi.org/10.1016/j.marpetgeo.2024.106752
Received 11 December 2023; Received in revised form 6 February 2024; Accepted 8 February 2024
Available online 9 February 2024

paleoecological context over a considerable period of time.

The spectral gamma-rays (SGR) give indications of the concentration of potassium (K), uranium (U), and thorium (Th) in rocks; they are routinely used for reconstructing the lithology, paleoenvironment, and paleoclimate of a measured succession (e.g., Bessa, 1995; Wignall and Twitchett, 1996; Bessa and Hesselbo, 1997; Ruffell and Worden, 2000; Dypvik and Harris, 2001; Schnyder et al., 2006; Basu et al., 2009; Kouamelan et al., 2020).

In the last few years, several studies have focused on testing the sensitivity of spectral gamma-rays (SGR) to reconstruct the paleoclimate based on changing lithological data derived from clay mineral variation content (Ruffell and Worden, 2000; Schnyder et al., 2006; Kouamelan et al., 2020). Taking advantage of the knowledge about different previously documented geochemical and paleoecological proxies, together with the data provided by the SGR, it is possible to reconstruct a paleoenvironment, characterizing the Th/K and Th/U ratios that show a trend in different sections, suggesting that both ratios indicate a paleoclimatic signal.

Analysis of SGR has been compared with XRF (X-ray fluorescence spectrometry) and XRD (X-ray diffraction) to analyze the content of clay minerals in different studied sections worldwide (e.g., XRF: Ruffell and Worden, 2000; Day-Stirrat et al., 2021; and XRD: Deconinck et al., 2003; Schnyder et al., 2006; Hesselbo et al., 2009; Paredes et al., 2020; Reolid et al., 2020). The correlation between SGR and clay mineralogy analysis (any of the previously mentioned methods) suggests a common control for their variation, making the SGR a good tool for the interpretation of the climatic signal considering the responses of other proxies. Furthermore, another application of the SGR is the recording of coarsening and

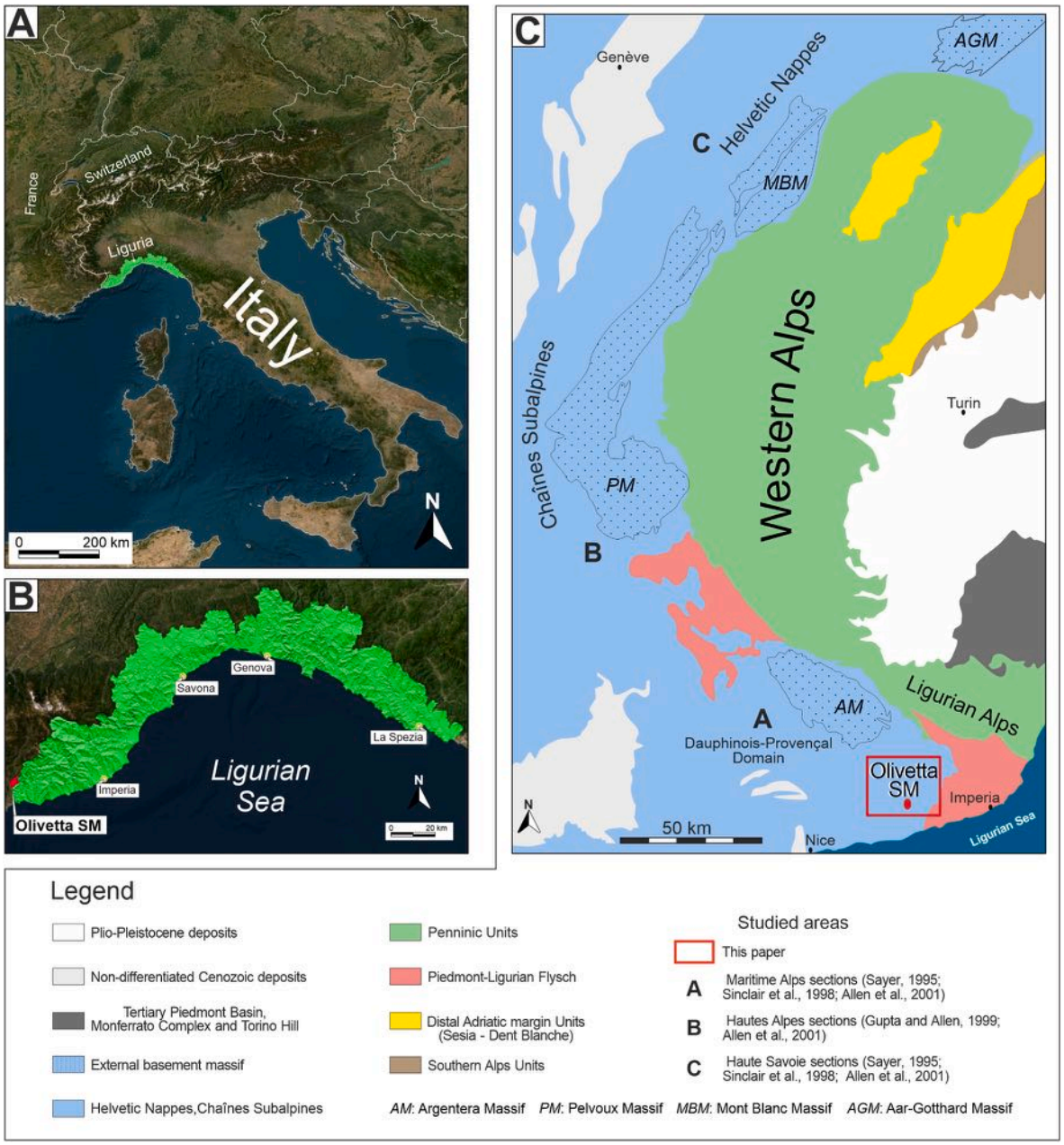

Fig. 1. A. Detailed location map of Italy showing the Liguria region (modified from https://server.arcgisonline.com/ArcGIS/rest/services/World_Imagery). **B.** Regional map of Liguria displaying the town of Olivetta San Michele (modified from https://server.arcgisonline.com/ArcGIS/rest/services/World_Imagery) **C.** Geological map of the Western Alps and adjacent domains, modified and simplified from Handy et al. (2010) and Di Capua et al. (2021) indicating the Olivetta San Michele section.

fining trends, which reflect sea-level regressions and transgressions in the stratigraphical sequences (Bendias and Aigner, 2015; Wethington and Pranter, 2018). The identification of cyclicity in the carbonate and siliciclastic deposits is based on a method that finds trends along stratal stacking patterns in the sedimentary record (e.g., Catuneanu, 2022). This approach helps to understand the evolution of sedimentation through space and time in a sedimentary basin. The marked cyclicity recorded in the French-Italian Maritime Alps and the France-Switzerland border within an overall deepening scenario indicates variations in sea level during the Eocene transgression, where old structures originated topographic lows in which the Microcodium Formation (Infranummulitic Formation) was deposited and then continued with a subsidence-caused transgression and the establishment of the carbonate ramp recorded by the Capo Mortola Calcarenite Formation (Nummulitic Limestones Formation) (Allen et al., 1991, 2001; Sayer, 1995; Sinclair et al., 1998; Varrone and Clari, 2003). Each cycle reflects the thickness and duration of specific facies, which in turn are the expression of the complex local interplay of the deposition of carbonate and siliciclastic deposits. In the French-Italian Maritime Alps, between 4 and 6 cycles of aggradational and progradational nature were recorded prior to the complete drowning of the ramp, showing that stacking patterns vary from place to place in the Alpine foreland (Sayer, 1995; Sinclair et al., 1998; Allen et al., 2001).

The present study focuses on the Paleogene carbonate-siliciclastic

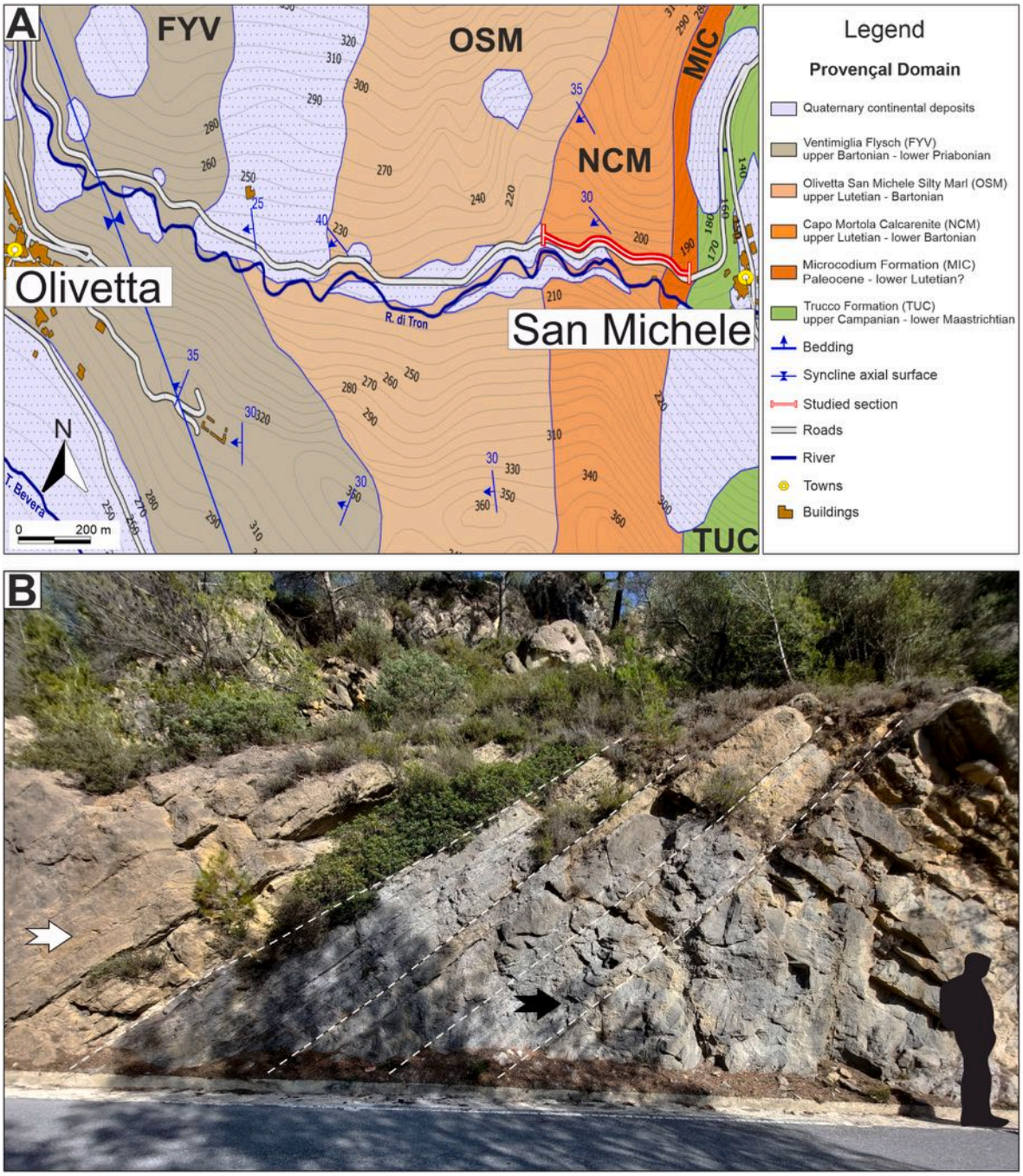

Fig. 2. **A.** Simplified geological map of the Olivetta San Michele area, showing the studied section; modified from Dallagiovanna et al. (2012a, b). **B.** Panoramic view of the Olivetta San Michele outcrop showing the Capo Mortola Calcarenite Formation (Bartonian). The white arrow shows a packstone interval (from 67.0 to 77.50 m), whereas the black arrow marks a wackestone layer (from 57.0 to 67.0 m) that corresponds to the long cycle II.

succession that crops out in northwest Italy (Olivetta San Michele, Liguria Region; Fig. 1A and B). The aims are: 1) to report the results of a high-resolution outcrop-based spectral gamma-ray (SGR) survey of exposed succession; 2) to decipher the paleoclimate derived from the SGR ratios that identify clay minerals; 3) to subdivide the sequence into different lithofacies using the SGR data and the available lithology; 4) to identify stacking pattern cycles derived from the log attributes of the SGR and their corresponding lithotypes; and 5) to demonstrate that the carbonate-siliciclastic succession can be correlated on a regional scale through the marked cyclicity with other sections in the French-Italian Maritime Alps and the France-Switzerland border prior to the drowning of the ramp.

2. Geological setting and studied section

The sector of the French-Italian Maritime Alps, which corresponds to the southeastern ending of the Dauphinois-Provençal Domain, represents a sector at the outer part of the continental margin of Europe (Fig. 1 A–C). The Mesozoic succession was deposited on the European margin between the opening and the beginning of the closure of the Tethyan Ocean (Sinclair et al., 1998; Varrone and d'Atri, 2007; Varrone and Decrouez, 2007). During the early stages of subsidence in the underfilled Alpine foreland basin, the Paleogene sediments of the Dauphinois Provençal Domain were deposited (Allen et al., 1991). The main characteristic of these deposits is their carbonate and siliciclastic origin (Fig. 2C), which are found not only in the French-Italian Maritime Alps but also in France and the France-Switzerland border (Allen et al., 1991, 2001; Sinclair et al., 1998; Varrone and Clari, 2003; Ferràndez-Cañadell et al., 2023).

The tectonic structure of this area is largely due to the deformation history spanning from the Cretaceous to recent times. The Pyrenean-Provençal orogeny structures (Upper Cretaceous) are involved in late Alpine folding and thrusting events (upper Eocene - lower Oligocene) linked to the moving of the Alpine orogenic wedge; the obtained structure has been involved in the contractional and extensional deformations mainly related to the counterclockwise rotation of the Corsica-Sardinia Block (Miocene) and, finally, affected by the Pliocene to recent extensional faulting (Gèze et al., 1968; Lanteaume, 1968; Lemoine et al., 1986; Gèze and Nestéroff, 1996; Martín-Martín et al., 2001; Ford et al., 2006; de Graciansky et al., 2010; Giammarino et al., 2010; Dallagiovanna et al., 2012a, 2012b; Seno et al., 2012; Decarlis et al., 2014; Morelli et al., 2022).

The Provençal Domain succession was uplifted at the end of the Cretaceous by the Pyrenean-Provençal orogeny and remained exposed to a strong, extensive erosion during the uppermost Cretaceous and the early Paleogene; this event produced a widespread unconformity at the top of the Cretaceous deposits (Lanteaume, 1968; Campredon and Giannerini, 1982; Apps et al., 2004; de Graciansky et al., 2010; Giammarino et al., 2010; Dallagiovanna et al., 2012a, 2012b; Seno et al., 2012; Marini et al., 2022; Briguglio et al., 2024). This domain evolved in a foreland-foredeep system during the Eocene thrusting of the orogenic wedge of the Western and Ligurian Alps onto this part of the European plate. This phase caused the deposition of the marine "Priabonian Trilogy" of Boussac (1912); this trilogy was named "Nummulitique" by Lanteaume (1968) and revised by Sinclair (1997, Sinclair Trilogy), comprising shallow-water limestones grading to deep-water marls covered by siliciclastic turbidite sedimentation that represent the Eocene fill of the foredeep basin (Lanteaume, 1968; Varrone, 2004; de Graciansky et al., 2010; Giammarino et al., 2010; Dallagiovanna et al., 2012a, 2012b; Seno et al., 2012; Marini et al., 2022). The Boussac's trilogy unconformably rests on Upper Cretaceous marly limestones (Trucco Formation), and it is composed of a transgressive lower complex capped by a turbiditic upper complex (Lanteaume, 1968; Campredon, 1977; Varrone, 2004; Giammarino et al., 2009, 2010; Dallagiovanna et al., 2012a, 2012b; Perotti et al., 2012; Seno et al., 2012; Maino and Seno, 2016; Mueller et al., 2020; Marini et al., 2022).

The lower complex is formed by many different siliciclastic, mixed and carbonate shallow marine lithofacies (Fig. 2A and B), reflecting the various paleogeographic settings affected by the transgression (Capo Mortola Calcarenite; upper Lutetian - lower Bartonian, according to the more recent literature) grading upwards to hemipelagic blue marls and brownish silty-marls with interbedded sandy bodies (Olivetta San Michele Silty-Marl; upper Lutetian? - lower Priabonian, according to the more recent literature) (Lanteaume, 1968; Campredon, 1977; Varrone, 2004; Giammarino et al., 2009, 2010; Dallagiovanna et al., 2012a, 2012b; Perotti et al., 2012; Seno et al., 2012; Maino and Seno, 2016; Mueller et al., 2020; Coletti et al., 2021; Marini et al., 2022; Briguglio et al., 2024). The upper complex includes siliciclastic turbidite deposits (Ventimiglia Flysch: upper Bartonian – lower Priabonian) fed by the erosion of Sardinia-Corsica and Maures-Esterel crystalline massifs and represents the foredeep basin late filling phase (Lanteaume, 1968; Varrone, 2004; Giammarino et al., 2009, 2010; Dallagiovanna et al., 2012a, 2012b; Perotti et al., 2012; Seno et al., 2012; Maino and Seno, 2016; Mueller et al., 2020; Marini et al., 2022).

The Olivetta San Michele section (Olivetta SM; Fig. 1. B, C, 2 A) is measured along the eastern limb of the asymmetrical, non-cylindrical, NNW-SSE-oriented syncline of Piène-Olivetta San Michele that represents the northernmost part of the structural complex of the 'Arc de la Roya' (Lanteaume, 1968; Gèze et al., 1968; Gèze and Nestéroff, 1996; Campredon, 1977; Giammarino et al., 2010; Dallagiovanna et al., 2012a, 2012b; de Graciansky et al., 2010; Seno et al., 2012; Decarlis et al., 2014; Marini et al., 2022). In this syncline are involved Upper Cretaceous to upper Eocene sedimentary rocks that are part of the succession of the eastern part of the southern Provençal paleogeographic domain (Giammarino et al., 2009; Giammarino et al., 2010; Dallagiovanna et al., 2012a, b; Perotti et al., 2012; Seno et al., 2012; 1C).

The Olivetta San Michele section is composed, bottom to top, of a) Upper Cretaceous marls and marly limestone (Trucco Formation; Fig. 2 A), b) *Microcodium*-rich, burrowed marls with greyish to reddish patches (Microcodium Formation; Fig. 2 A), c) fine to coarse grained siliciclastic, mixed and carbonate deposits of shallow marine environment (Capo Mortola Calcarenite Formation; Fig. 2 A, B; 3), d) hemipelagic silty marls and marls (Olivetta San Michele Silty Marl; Fig. 2 A), e) siliciclastic turbidite deposits (Ventimiglia Flysch; Fig. 2 A) (Lanteaume, 1968; Campredon, 1977; Varrone, 2004; Giammarino et al., 2009, 2010; Dallagiovanna et al., 2012a, 2012b; Perotti et al., 2012; Seno et al., 2012; Maino and Seno, 2016; Brandano, 2019; Mueller et al., 2020; Coletti et al., 2021; Marini et al., 2022; Briguglio et al., 2024).

The Olivetta San Michele lithostratigraphic section fits with the typical succession of this part of the Provençal Domain (Fig. 1 C), including the *Microcodium*-rich lithofacies (Microcodium Formation), the whole transgressive event (deposited on the weathered Upper Cretaceous rocks), and the Ventimiglia Flysch Formation. The Microcodium Formation is interpreted as the result of strong weathering, reworking, and/or deposition in subaerial, lagoonal, and estuarine environments of the Upper Cretaceous deposits, and it is referred to as the Paleocene-lower Lutetian in the more recent literature (Lanteaume, 1968; Varrone and Clari, 2003; Giammarino et al., 2010; Dallagiovanna et al., 2012a, 2012b; Seno et al., 2012; Coletti et al., 2021).

3. Material and methods

In this study, a total of 223.3 m of sedimentary succession of the Olivetta SM was studied along the Paleogene intervals, covering the Microcodium Formation, and the Capo Mortola Calcarenite Formation (Fig. 2A and 3). Spectral gamma-rays measured for this study along the succession are coupled with lithology, grain size, texture (following Grabau, 1904; Flügel, 2012), biogenic components, sedimentary structures, and ichnofabrics, as published by Arena et al. (2024).

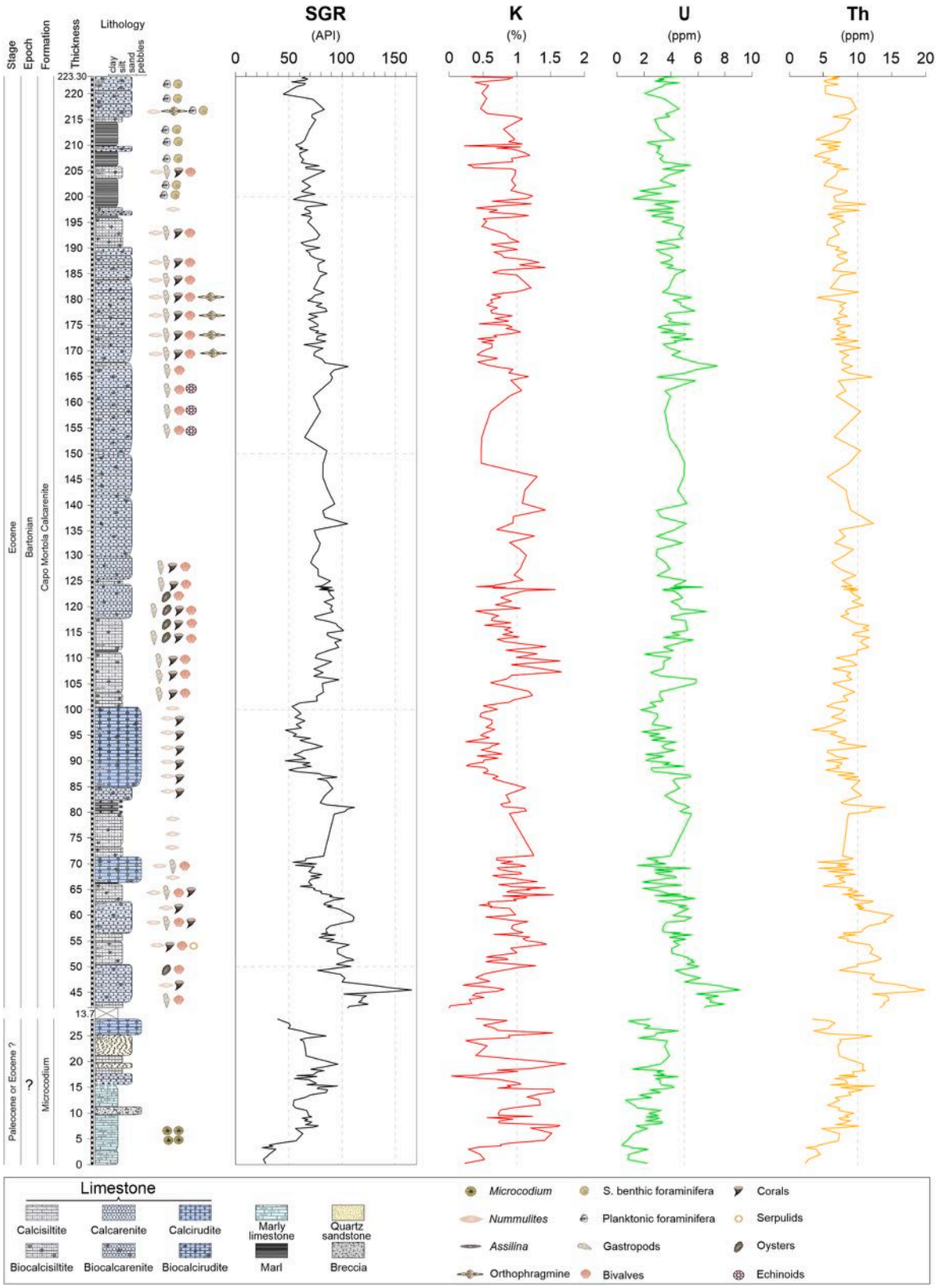

Fig. 3. Lithology, fossil content (data on the Capo Mortola Calcarenite Formation modified after Arena et al., 2024), and spectral gamma-ray data divided in total SGR (API), potassium (K%), uranium (U ppm), and thorium (Th ppm) of the Olivetta San Michele section.

3.1. Spectral gamma-ray

A total of 340 sampling points were measured for spectral gamma-ray (SGR) along the Olivetta SM using a Codevintec Gamma Ray Surveyor Vario (VN6 Nal (Ti)), with sampling intervals at around 25–30 cm whenever possible (Fig. 3). The detector was placed following the stratification on a flat and fresh rock surface, with measurements lasting 3 min per point.

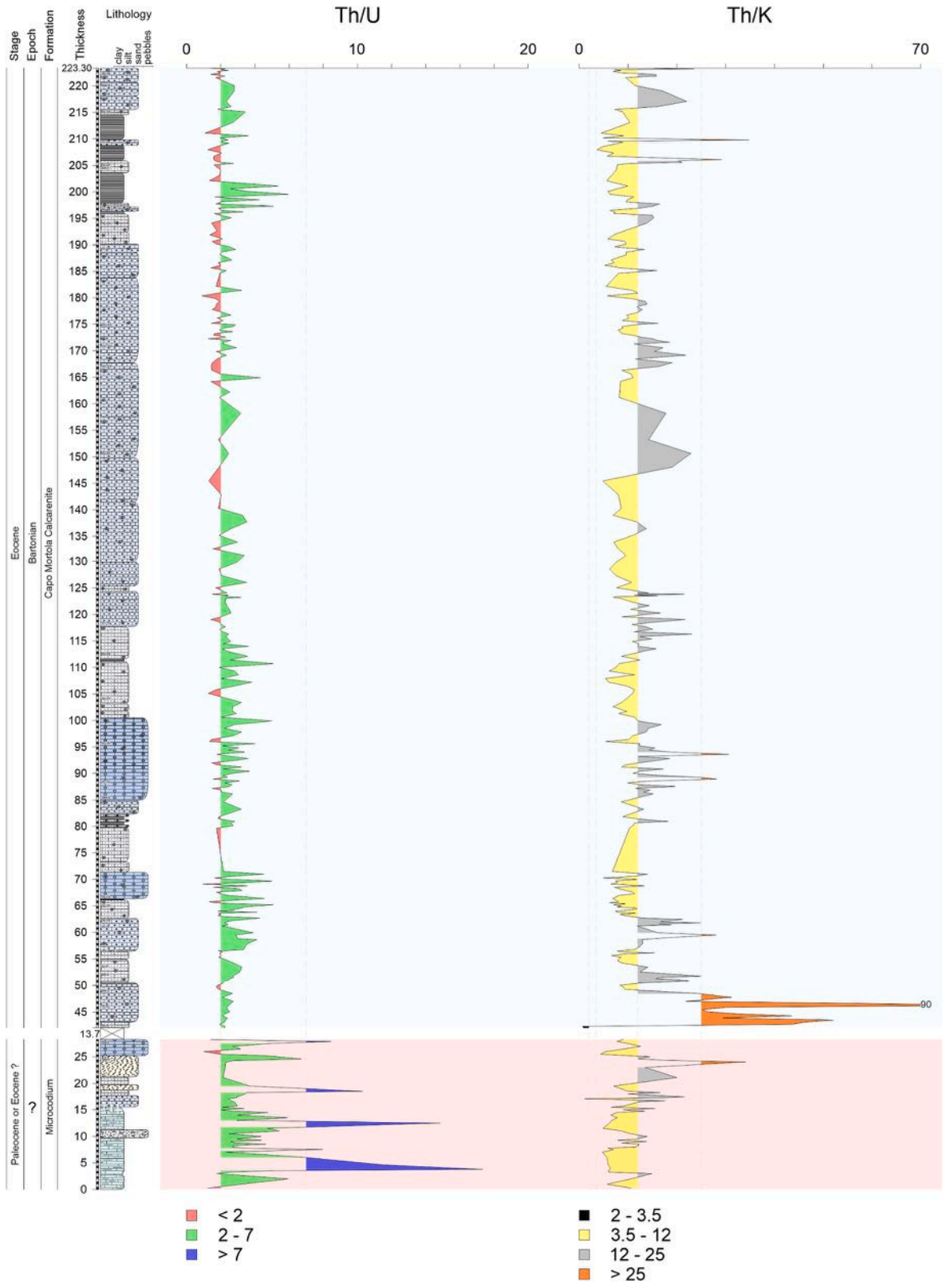

Fig. 4. Lithology of the Olivetta San Michele section correlated with the Th/U and Th/K ratios (light red shadow band: normal marine and continental conditions; light blue shadow band: normal marine conditions).

The SGR log measures the natural gamma radiation emanating from a source, splits into contributions from each of the major radio-isotopic sources (Glover, 2000), the radioactivity emitted by potassium (K), uranium (U), and thorium (Th), and therefore provides the natural gamma ray count concentration in rocks, which can be measured non-destructively and in real time, both in an outcrop and in a borehole (Slatt et al., 1992; Ruffell and Kürschner, 2020). The natural gamma radiation is emitted from the decay of mineral-hosted ^{238}U, ^{232}Th, and ^{40}K radioisotopes and presents specific energy levels unique to each isotope. The spectrometer automatically reports the dose rate in nanogray per hour (nGy/h), and the concentrations of U and Th are given in parts per million (ppm), while K is expressed in percentage (%). The SGR values were calculated from the spectral values using the formula (Doveton, 1994; Luthi, 2001; Ellis and Singer, 2007). SGR [API] = K [%] x 16 + U [ppm] x 8 + Th [ppm] x 4 to scale the counts of the SGR in terms of the API (American Petroleum Institute) gamma ray unit, which is used for all modern records (Fig. 3).

Based on these concentrations, it is possible to calculate the Th/U and Th/K ratios (Fig. 4), which are used to analyze depositional environments and identify clay minerals. Because of the strong relationship between changes in depositional environments and sedimentary processes, the Th/U ratio is a useful proxy for indicating paleoredox conditions (e.g., Adams and Weaver, 1958; Wignall and Twitchett, 1996; Basu et al., 2009; Kouamelan et al., 2020). High Th/U ratios are interpreted as having a continental origin (Th/U > 7) and are associated with oxidizing conditions in the water column, while low values (Th/U < 2) are related to marine reduced settings and anoxic water conditions. Transitional periods between oxidizing and reducing environments, associated with less oxic to dysoxic conditions, are represented in marine normal settings by Th/U ratios ranging from 2 to 7 (e.g., Adams and Weaver, 1958; Cowan and Myers, 1988; Wignall and Twitchett, 1996; Ruffell and Worden, 2000; Dypvik and Harris, 2001; Fabricius et al., 2003; Basu et al., 2009; Kouamelan et al., 2020; Cao et al., 2021). The thorium-potassium ratio (Th/K) was calculated to determine the type of clay mineral content in rocks (e.g., Schlumberger, 1997).

3.2. Log-attribute analysis

Other applications of the gamma ray (GR) are given by the recorded patterns of decreasing-upward and increasing-upward curves that may indicate coarsening and fining trends associated with sea-level regressions and transgressions to reconstruct the stratigraphical sequences (Bendias and Aigner, 2015; Wethington and Pranter, 2018). Attribute analysis has been used to study well-log data because it allows the identification and highlight of log signals that are geologically significant in an automated fashion (Wethington and Pranter, 2018; Henglai, 2018). This study examines log attributes, referred to as derivative trend analysis (DTA), that are applied to the GR (Fig. 5). The first step of the DTA process is to filter the log data (Gaussian smoothing function) to the appropriate frequency for the investigation at hand using the PAST software version 4.1 (Hammer et al., 2001). The filter attenuates high-frequency noise while preserving lower-frequency trends, resulting in smoothed log curves. Smoothed curves are then differentiated using the central-difference method (Wethington and Pranter, 2018):

derivative (i) = (GR [i+1] – GR [i-1])/(depth [i+1] – depth [i-1])

This method mainly calculates the slope between neighboring points on a curve to estimate the derivative of the point of interest. After the derivative at each point of the Olivetta SM is calculated, the resulting curve shows positive values when the original curve is decreasing upward and negative values when the original curve is increasing upward. (Fig. 5).

3.3. Lithofacies determination

Key lithologies of the Olivetta SM section were identified through detailed lithological descriptions. Outcrop descriptions include observations of primary lithology, grain size, sedimentary structures, and ichnofabrics. All these data are combined with the data performed with the SGR trend of stacking patterns (retrogradation, progradation, and aggradation) and log-attributes of the SGR to determine the lithofacies of the Olivetta SM section (Fig. 5).

Thin section analysis was conducted on a custom-made Optech GZ808 optical stereomicroscope with a Delta Pix by Invenio (model 6EIII) digital camera, used to take photos of different samples. A total of 14 rock samples (from OL-1 to OL-14; two thin sections for each rock sample) in the interval from 0 m to 28.30 m were analyzed in this study to complete the set of the thin sections (71) of the whole studied succession (Supplementary Table S1). From 42 m to 223.30 m, the microfacies analyses were previously described and published by Arena et al. (2024). The textural classification of the thin sections follows the scheme of Dunham (1962), and the biogenic components were identified when possible. The main characteristics used to describe the rock are the percentage of matrix, the abundance of skeletal components (when possible), grain roundness, grain sorting, the presence of quartz, glauconite, and organic matter, and special features such as diagenesis, bioturbation, deformation, and transport evidence. For the fossil content, the matrix includes abundance data (0 = absent, 1 = common, 2 = abundant) on smaller benthic foraminifera, planktonic foraminifera, and *Microcodium* (Supplementary Table S1).

4. Results

4.1. Spectral gamma-ray of the Olivetta SM section

The calculated spectral gamma-ray (SGR) in API units varies from 23.04 to 165.04 (Fig. 3). The lowest SGR values (from 23.04 to 37.72 API) are especially recorded at the base and top of the Microcodium Formation (from 0.25 m to 4.0 m; and sample 28.30). Values of SGR greater than 100 API are mainly observed at the base of the Capo Mortola Calcarenite Formation (from 42 m to 46 m and from 50.60 m to 51.50 m), with some exceptions in the middle and top of the studied section (Fig. 3).

Emissions of the three isotope elements of the SGR display a marked variation throughout the whole section (Fig. 3). Variations in K (%) values range between 0 and 1.7% in the whole stratigraphic succession (Fig. 3). Most values of K fluctuate between 0.5% and 1%, whereas values above 1% and less than 0.5% are sporadically recorded throughout the whole section (Fig. 3).

The concentration of U ranges between 0.23 and 9.08 ppm (Fig. 3). Most values of U display concentrations between 2 and 4 ppm, but values greater than 4 ppm are recorded in the Capo Mortola Calcarenite Formation, especially at its base (Fig. 3). Although values less than 2 ppm are found throughout the section, most of them are recorded in the Microcodium Formation (Fig. 3).

The concentration of Th varies between 2.07 and 19.90 ppm (Fig. 3); most values range between 5 and 10 ppm, covering the whole stratigraphical succession. Some samples, especially at the base of the Microcodium Formation, display a significant decrease in the concentration of Th (<5 ppm), whereas an increase in the concentration of Th greater than 10 ppm is recorded in the Capo Mortola Calcarenite Formation, especially at its base (Fig. 3).

The Th/U ratio displays a range between 0.70 and 17.30, with common values varying between 2 and 7 in almost the entire studied section but being more dominant in the Microcodium Formation than the Capo Mortola Calcarenite Formation (Fig. 3). Values of the Th/U ratio <2 are recorded throughout the section, but these values are recorded with major frequency at the top of the Capo Mortola Calcarenite Formation. That contrasts with values of the Th/U ratio >7, which are mainly observed in the Microcodium Formation (Fig. 4).

The Th/K ratio fluctuates between 0 and 90 (Fig. 4). Most of the values of the Th/K ratio are between 3.5 and 12 in the entire stratigraphic succession, followed by values that are in the range of 12 and 25.

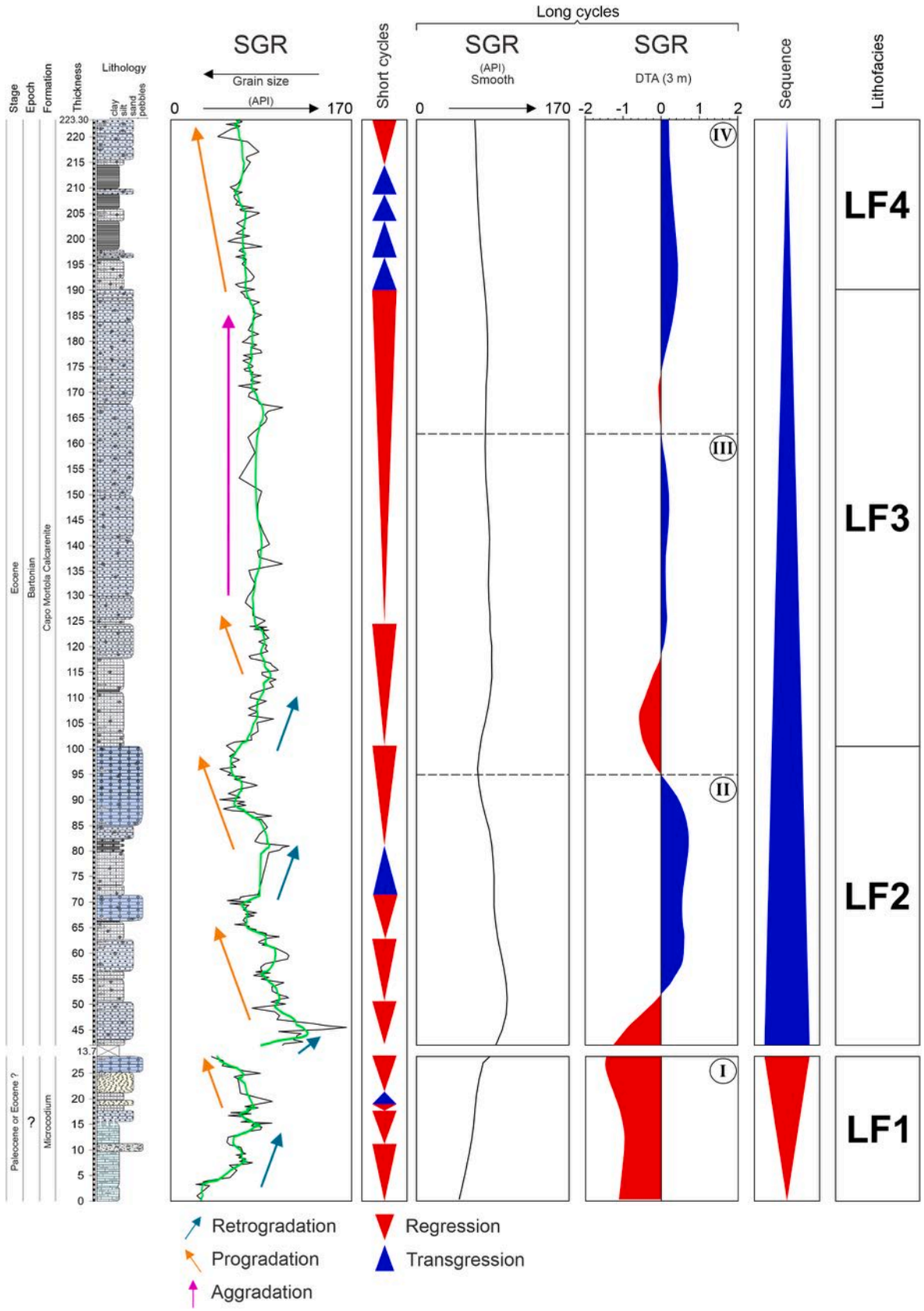

Fig. 5. Sequence stratigraphic interpretation of the SGR displaying the inferred lithofacies (on the right side) of the Olivetta San Michele section. The track on the left is a regular SGR (API) curve indicating the progradational, retrogradational, and aggradational stacking patterns (black curve: SGR data; green curve: three-point moving average). The next track displays the short cycles characterized by regressive and transgressive patterns. The third and fourth tracks represent the long cycles that are calculated according to the derivative trend analysis (DTA). The fifth track is a sequence that represents the Bartonian marine transgression.

The former values are observed more frequently in the Capo Mortola Calcarenite Formation, especially at its base. In turn, the Th/K ratio values >25 are recorded in sporadic samples in both formations, but at the base of the Capo Mortola Calcarenite Formation, these values are constant in the interval from 42 m to 47.50 m (Fig. 4).

4.2. Log-attribute of the SGR

The Microcodium Formation and the Capo Mortola Calcarenite Formation were deposited in different environments that show different signals of the SGR, allowing us to distinguish the increase and decrease in the grain size of the rocks in the opposite direction to the decrease and increase of the SGR signal in API (Fig. 5). According to these trends in the SGR signal of the lithology, three different patterns are recognized that point out progradation (coarsening-upward), retrogradation (finning-upward), and aggradation in the Olivetta SM section. From the base to the top of the section are recorded five intervals of fining upward, four intervals of coarsening upward, and one interval of aggradation (Fig. 5).

Nevertheless, common stacking patterns based on lithology that record an overall trend of progradation rather than aggradation and retrogradation, are recognized throughout the studied section, allowing for the recognition of short and long cycles and displaying an understandable configuration of the strata during the evolution of the sedimentary basin (Fig. 5). Cycle sets are very well reflected in the SGR patterns and by clear lithological trends, while in the short cycles, three complete cycles (regressive-transgressive) and eleven half cycles (regressive or transgressive) are identified (Fig. 5).

The application of the DTA (derivative trend analysis; Wethington and Pranter, 2018) on the SGR signal of the Olivetta SM section is carried out every 3 m to ensure that this interval covers the trend of the curve completely (Fig. 5). After applying the Gaussian smoothing function filter, the curve result shows a very smooth signal with a poorly defined tendency to attenuate high-frequency noise. Subsequently, when calculating the first derivative of the curve (long cycle; Fig. 5), it is possible to distinguish three complete cycles (regressive-transgressive; II, III, and IV), especially in the Capo Mortola Calcarenite Formation, and a half cycle (regressive; I) in the Microcodium Formation (Fig. 5). In this study, low SGR values indicate grain-size pebbles and sandstone, while high SGR values represent claystone. The positive trend of the DTA means an upward decrease of SGR values, suggesting cleaning upward patterns with a decrease in clay content, while a negative trend indicates an upward increase in SGR values, showing a fining-upward motif with an increase in clay content (Fig. 5).

4.3. Lithofacies of the Olivetta SM section

Based on data previously published by Arena et al. (2024) and the new data provided in this study about the SGR records, it is possible to recognize four lithofacies (LFs) in the mixed carbonate-siliciclastic system recorded both in the Microcodium Formation and the Capo Mortola Calcarenite Formation (Fig. 4; Supplementary Table S1). Unlike the study carried out by Arena et al. (2024), where both the macro- and microfacies of the Capo Mortola Calcarenite Formation were addressed in greater depth with special attention to the fossil content, the LFs defined in this study are based mainly on the variation of the grain size that records the coarsening-upward, fining-upward, and aggradation stacking patterns that also distinguished both outcrop descriptions and the SGR signal. The studied formations consist predominantly of limestones, which are differentiated in their granulometric character (calcirudite, calcarenite, and calcisiltite), and in a minor role by marls, marly limestone, quartz sandstone, and breccia (Figs. 3–5). Each LF can display significant variability, mainly due to its fossil content, which belongs to a specific environment (Supplementary Table S1).

LF1 is within the Microcodium Formation and is organized in coarsening-upward and fining-upward stacking patterns that correspond to a long cycle I (Fig. 5; Supplementary Table S1). This LF is made up of marly limestone, breccia, quartz sandstone, calcirudite, calcarenite, and calcisiltite, as confirmed by the analyzed thin sections, mudstone, wackestone, and quartz sandstone. Within the first few centimeters of the marly limestones, some reworked planktonic and benthic foraminifera may be recorded in thin sections (mudstone). Subsequently, records of *Microcodium* were observed in some layers of the same lithology and the respective thin section (mudstone) (Supplementary Table S1).

LF2 is composed of coarsening-upward and fining-upward stacking patterns associated with long cycle II (Fig. 5; Supplementary Table S1). A gradation of calcirudite, calcarenite, calcisiltite, and marl with fossil content is recorded in this LF of the Capo Mortola Calcarenite Formation. Thin sections determined a variation between bioclastic wackestone and bioclastic packstone within this LF (see Arena et al., 2024).

LF3 is established by coarsening-upward stacking patterns associated with long cycle III (Fig. 5; Supplementary Table S1). Calcarenite, calcisiltite, and marl are recorded in this LF (Capo Mortola Calcarenite Formation) with different abundances and diversity in the fossil content. Bioclastic wackestone and packstone characterized this LF (see Arena et al., 2024).

LF4 is characterized by fining-upward and coarsening-upward stacking patterns associated with long cycle IV (Fig. 5; Supplementary Table S1). The lithology typical of this LF is given by layers of calcarenite, calcisiltite, and marl (Capo Mortola Calcarenite Formation) with abundant fossil content that correspond to bioclastic mudstone, wackestone, and packstone (see Arena et al., 2024).

5. Discussion

5.1. Response of the spectral gamma-ray

The moderate-high SGR values recorded in the carbonate ramp in the Olivetta SM section, which are associated with U, Th, and K and their calculated Th/U and Th/K ratios, fluctuate under different controls such as clay mineral content, paleo-redox conditions, and paleoclimate (e.g., Ruffell and Worden, 2000; Hesselbo et al., 2003; Ruffell et al., 2006; Gao et al., 2018; Kouamelan et al., 2020). The comparative behavior of K, U, and Th with the total gamma radiation of the stratigraphic succession suggests that these elements are varying, influencing the total count of the SGR (API) in a very similar way. This is confirmed by the poor correlation between the total gamma count and K (Fig. 6A), whereas U and Th show a high correlation with the total gamma count, especially the latter (Fig. 6A and B). The increase in Th content may also be related to the detrital input, which is mainly located in oxides and silicates and is less mobile than U under oxidizing conditions (Myers and Wignall, 1987; Mernagh and Miezitis, 2008). Due to the high correlation of Th and U and the low correlation of K, the calculated Th/U and Th/K ratios display the influence of these elements in their interpretation (Figs. 4 and 6D, E).

5.1.1. Paleoclimatic implications in the Olivetta SM section

The Th/K ratio is used as a weathering index because it is possible to contrast their concentrations with their chemical reactions as they are weathered. It is known that Th is an immobile element, insoluble in natural water, and concentrated in residual minerals, unlike K, which is a highly soluble element that is leached from sediments rich in feldspars and muscovite (Myers, 1987; Chamley, 1989; Schnyder et al., 2006). In turn, potassium is an important component of feldspars, mica, and illite, but it is absent in kaolinite, a mineral formed by the hydrolysis of aluminosilicates under humid climate conditions (Myers, 1987). Thus, the Th/K ratio depends on the genesis of clay mineral assemblages, which is in turn influenced by climatic fluctuations (e.g., Quirein et al., 1982; Bessa, 1995; Ruffell and Worden, 2000; Fabricius et al., 2003; Gao et al., 2018; Kouamelan et al., 2020).

The determination of clay mineral content is based on the cross-plot of the Th/K ratio, where minerals such as chlorite, glauconite, illite,

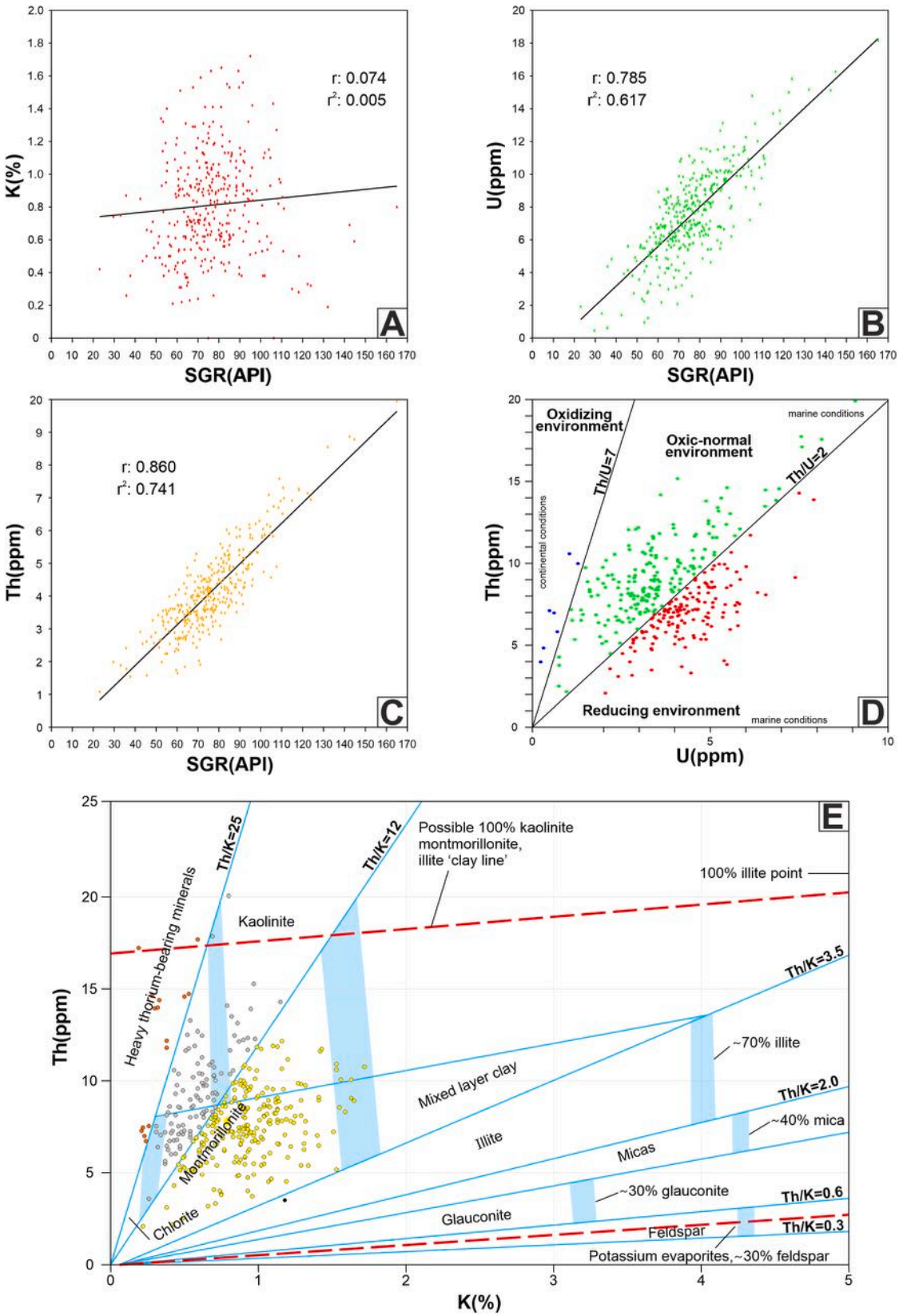

Fig. 6. A. Cross-plot of K (%) vs. SGR (API). **B.** Cross-plot of U (ppm) vs. SGR (API). **C.** Cross-plot of Th (ppm) vs. SGR (API). **D.** Cross-plot of Th/U showing transitional periods among oxidizing, oxic-normal, and reducing conditions corresponding to marine and continental environments of the Olivetta San Michele section. **E.** Cross-plot of Th/K displaying different clay mineral content in the Olivetta San Michele section based on the Schlumberger chart (Schlumberger, 1997): Th/K ratio 2–3.5: Illite; Th/K ratio 3.5–12: Smectite (Montmorillonite); Th/K ratio 12–25: Kaolinite; Th/K ratio >25: heavy thorium-bearing minerals.

kaolinite, and smectite (montmorillonite) have a certain range of values to differentiate themselves (e.g., Schlumberger, 1997). Thus, Th/K values greater than 25 are associated with heavy Th-bearing minerals, and Th/K values between 12 and 25 are linked with kaolinite. In contrast, intermediate Th/K values (between 3.5 and 12) are related to montmorillonite (smectite), whereas low Th/K values (from 2.0 to 3.5) are linked with illite (e.g., Schlumberger, 1997, Figs. 4 and 6E).

In the Olivetta SM section, smectite (montmorillonite) is the most abundant clay mineral, followed by kaolinite, whereas heavy thorium-bearing minerals are recorded as traces throughout the studied section, according to the cross-plot (Fig. 6E). These clay minerals are known to be controlled by climatic variations (Bessa, 1995; Kouamelan et al., 2020); smectite (montmorillonite) is typically formed by chemical weathering of soils in warm to temperate climates where seasonal climate fluctuations are associated with humid or arid regimes (e.g., Deconinck, 1992; Diester-Haass et al., 1998; McKinley et al., 2003; Kennedy and Wagner, 2011). Kaolinite is associated with tropical soils that are the result of highly hydrolytic weathering, where K is removed from the soil profile (e.g., Robert and Chamley, 1991; Bessa, 1995; Chamley, 2001; Deconinck et al., 2003), and kaolinite is linked with humid climates and well-drained areas. Therefore, the Th/K ratio is higher during humid kaolinite-rich periods than during arid kaolinite-poor periods (Myers, 1987; Ruffell and Worden, 2000; Li et al., 2019).

The early Paleogene experienced the most pronounced long-term warming trend of the Cenozoic, characterized by transient warming events that affected the climate system and had especially negative consequences for the evolution of carbonate platforms (Zachos et al., 2001; Scheibner and Speijer, 2008; Martín-Martín et al., 2021). The Mediterranean region was influenced by diverse gradients of temperature within a greenhouse climate that alternated between a warm arid and a warm humid climate (e.g., Bolle and Adatte, 2001; Murru et al., 2003; Scheibner and Speijer, 2008; Spofforth et al., 2010; Giorgioni et al., 2019; Honegger et al., 2020; Messaoud et al., 2021; Peris-Cabré et al., 2023; Briguglio et al., 2024).

The evidenced changes between kaolinite and smectite in the Olivetta SM section may suggest a climatic influence where kaolinite reflects humid conditions over long dry periods where smectite dominated (e.g., Bessa, 1995; Hesselbo et al., 2009), being the result mainly from the local environmental conditions, but the common features seem to be controlled by regional fluctuations in a warm-humid climate and wet-dry seasonal alternations, as evidenced in the Mediterranean basins during the Paleocene and Eocene.

5.1.2. Marine and continental environments

The Th/U ratio is used to differentiate the marine versus continental provenance of the sediments (Myers, 1987; Ehrenberg et al., 2008). Values of the Th/U ratio generally falling below 7 suggest a prominent marine normal origin, whereas values higher than 7 indicate a fully continental provenance associated with typical oxidizing terrestrial settings (e.g., Schnyder et al., 2006; Kouamelan et al., 2020) (Figs. 4 and 6). The Th/U ratio in the Olivetta SM section remains on average within the range of marine oxic-normal conditions (values from 2 to 7); some samples with values less than 2 that have a marine origin are interpreted to belong to a reducing marine environment (e.g., Myers, 1987; Kouamelan et al., 2020).

Carbon content in a stratigraphic succession may influence thorium and uranium concentrations, reducing Th/U ratios (Adams and Weaver, 1958); nevertheless, gamma ray and TOC curves raise the possibility that uranium enrichment may be caused by changes in hydrodynamic regimes rather than productivity and terrigenous contribution in stable marine environments, characterized by a high carbonate content (Ehrenberg et al., 2008; Reuter et al., 2013; Briguglio et al., 2024). Instead, a marginal marine environment suggested by high Th/U ratios could possibly be controlled by low U rather than high Th (Figs. 4 and 6). Finally, the Th/U ratio in the Olivetta SM section indicates marine conditions, especially along the Capo Mortola Calcarenite Formation, whereas in the Microcodium Formation, high values of the Th/U ratio are interpreted as a transitional environment that fluctuated between marine and continental conditions (Figs. 4 and 6D).

5.2. Transgressive–regressive (T–R) cycles

The recognition of vertical stacking patterns to distinguish progradational, aggradational, and retrogradational cycles is independent of scale and control mechanisms. The character of lithofacies and cycle symmetry of individual carbonate cycles are controlled by local environmental conditions, including subsidence and eustasy (Crevello et al., 1991).

The approach of the sedimentary processes reflected in the lithology allows for the reconstruction of depositional systems in sedimentary basins formed in the most diverse tectonic settings, which can be interpreted according to the analysis of sequence stratigraphy (Catuneanu, 2019, 2022).

The local scale of a stratigraphic analysis can be based on outcrops, cores, and well logs, identifying stacking patterns through the vertical succession indicative of transgressive-regressive (T-R) cycles (e.g., Catuneanu, 2022). These cycles reflect the variations in the ratio between accommodation space (A) and sedimentation rates (S). The prograding phases correspond to periods with an A/S of <1 and the retrograding phases to periods with an A/S of >1 (Homewood et al., 2000).

In this study, the high-resolution sequence that forms the stratigraphic framework was defined according to the cyclic changes in the lithofacies associations that reflect the shoreline trajectory, which are organized by ascending and descending trends of the SGR that correspond to changes in grain size, clay content, and mineralogy, indicative of transgressive and regressive cycles in sedimentation, and whose stacking patterns are to be interpreted as part of larger sedimentary cycles, reflecting changes in sediment supply and relative sea level (e.g., Krassay, 1998; Catuneanu, 2022).

In the Olivetta SM section, the Microcodium Formation records the short cycles characterized by regressive and transgressive stacking patterns that, according to the DTA, are interpreted as a long regressive cycle I (regression; Figs. 5 and 7). According to different authors (e.g., Sinclair et al., 1998; Allen et al., 2001; Varrone and Clari, 2003), the Microcodium Formation corresponds to an environment of brackish lagoon-estuarine deposits, recording a passage between an environment of continental and paralic deposits that precedes marine transgression in the Maritime Alps (the Nummulitic Limestone Formation is equivalent to the Capo Mortola Calcarenite Formation).

In the Olivetta section, the Capo Mortola Calcarenite Formation is characterized by short cycles, alternating progradational, retrogradational, and aggradational stacking patterns that are grouped according to the DTA in three long cycles (II, III, and IV; Figs. 5 and 7). These small-scale cycles are composed of shallowing-upward cycles (coarsening-upward) prior to the drowning of the carbonate ramp. However, the short cycles reflected progradational and/or aggradational stacking patterns that accumulated during a relative sea level maximum, with a transition near the top of the succession showing evidence of the onset of retrogradation and deepening near the overlying marls (Fig. 5). Long-term variations in accommodation may be responsible for vertical restriction and variability in the formation of small-scale cycles (Lehrmann and Goldhammer, 1999; Peterhänsel and Egenhoff, 2008), which may be explained by lower-order sea level fluctuations with a larger amplitude (Vail et al., 1977; Haq et al., 1987). Like the sediments recorded in the Nummulitic Limestone Formation in France and the France-Switzerland border, they are also organized in shallowing-upward cycles, separated by rapidly deepening surfaces, in which the frequency, number, and total thickness vary from one place to another (Allen et al., 1991, 2001; see Table 1). This diachroneity is evident in the studies of the France-Switzerland border, the French

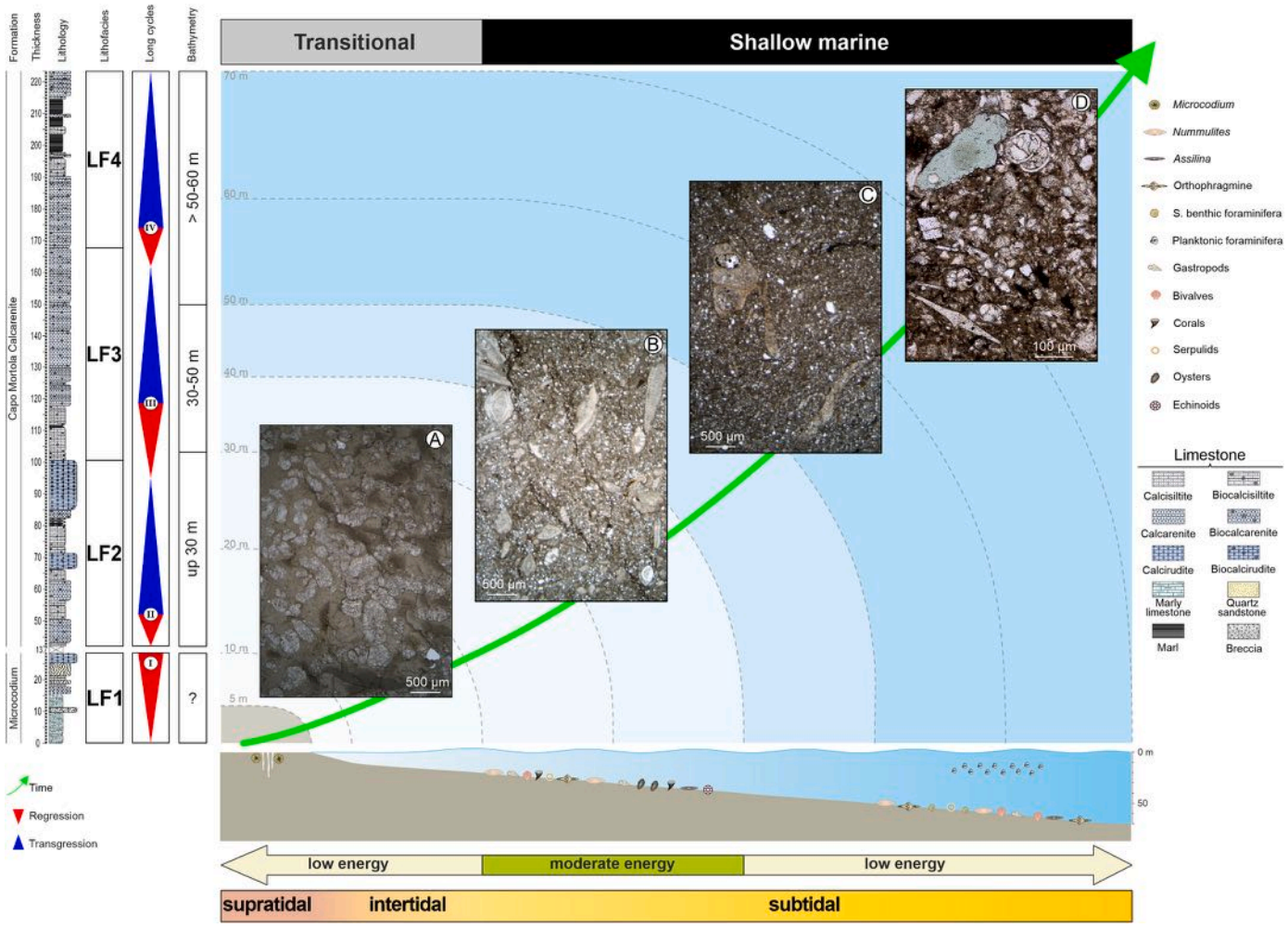

Fig. 7. Paleoenvironmental evolution of the carbonate-siliciclastic ramp at the Olivetta San Michele section in two dimensions. Thin sections show the variation of lithofacies upsection. **A.** Mudstone with *Microcodium* (5.5 m; Microcodium Formation). **B.** Packstone (87.0 m; Capo Mortola Calcarenite Formation). **C.** Wackestone (173.8 m; Capo Mortola Calcarenite Formation). D. Packstone (223.2 m; Capo Mortola Calcarenite Formation).

Table 1
Stacking patterns in the Nummulitic Limestone of the Foreland Basins of the Western Alps (Italy and France).

Location	Sections	Stratigraphic Unit	Cycles	References
Maritime Alps (Italy)	Olivetta SM	Capo Mortola Calcarenite	6 cycles	This study
Maritime Alps (France), northern synclines (Annot, Argens, Agneres)	northern synclines Ivoire Antonin	Nummulitic Limestone	4-6 cycles 6 cycles 8 cycles	Sayer (1995); Sinclair et al. (1998); Allen et al. (2001)
Hautes Alpes (France)	Crete de l'Arche	Nummulitic Limestone	7 wave cut platforms and risers	Gupta and Allen (1999); Allen et al. (2001)
Haute Savoie (France-Switzerland border), Thones syncline	Le Chinaillon	Nummulitic Limestone	8 cycles	Sayer (1995); Sinclair et al. (1998); Allen et al. (2001)

Maritime Alps, and in this study, where the different areas were deposited with similar sediments and cycles and key surfaces developed at different stages of the basin's development (Sayer, 1995; Sinclair et al., 1998). Long-duration cycles are preserved in Paleocene to mid-Eocene Nummulitic Limestone in Switzerland (Allen et al., 1991, 2001), whereas a larger number of shorter duration cycles are recorded in the middle Eocene of France, where the maximum number of shallow ascending cycles is divided into 6 and 8 before drowning of the carbonate ramp (e.g., Sayer, 1995; Sinclair et al., 1998; Allen et al., 1991, 2001). Six cycles recorded in the Olivetta SM section support a regional trend, where the number of cycles depended on whether the locality represented deposition at a structural maximum or at a corresponding minimum (Table 1). The aggradation and progradation of the Nummulitic Limestones in the western Alps reflect the sediment accumulation in the carbonate ramp at a rate similar to or greater than the rate of relative sea level rise associated with the flexural subsidence of the basin margin (Sinclair et al., 1998; Allen et al., 2001).

Transgressive cycles have also been recorded on other carbonate platforms during the middle Eocene (Bartonian) in the western Tethys, which were deposited in domains other than the Alps. Two minor transgressive depositional cycles are recorded in northern Morocco (Martín-Martín et al., 2023), as well as in the foreland basin of the southeastern Pyrenees (Spain), where two transgressive-regressive cycles are also recorded (Serra-Kiel et al., 2003; Castelltort et al., 2003; Martín-Martín et al., 2021). Both the lithological and fossil content

recorded in the western sections of Tethys and the sections of the Alps (this study) show similarities during the Bartonian, where the deepening of the carbonate ramps, due to transgression, allowed differentiation of cyclicity stacking patterns according to the tectonic domain of the basin. The sea level changes, combined with the effects of an increase or decrease in sediment supply and tectonic and climate control temperatures, exerted a response on the carbonate system in the evolution of a carbonate ramp in the Westen Tethys during the middle Eocene (e.g., Sayer, 1995; Sinclair et al., 1998; Allen et al., 2001; Serra-Kiel et al., 2003; Castelltort et al., 2003; Martín-Martín et al., 2021, 2023).

5.3. The evolution of the drowning ramp

The development of the carbonate ramp of the Olivetta SM section is marked by the evolution of the Ligurian Alps foredeep basins in the context of a westward migration of the foreland bulge and the start of a transgression, which occurred after an erosional unconformity, separating the Upper Cretaceous and the Paleocene-Eocene sedimentary deposits (Varrone, 2004; Giammarino et al., 2009; Decarlis et al., 2014).

The environmental deposition of the Microcodium Formation is assumed to have developed in a marine to marginal marine fan delta setting (Sinclair et al., 1998; Varrone and Clari, 2003). This is confirmed by the lithological variation of LF1 going from limestone and breccias to quartz sandstone, suggesting a deposition in an environment surrounding a fluvial source and close to the sea. Furthermore, *Microcodium*, widely accepted to originate in or around the roots of terrestrial plants that grow in carbonate-rich soils and/or subaerially exposed carbonate substrates (Molina et al., 2006; Kabanov et al., 2008, 2010; Rodríguez-Tovar et al., 2020), is observed in LF1 (Figs. 3 and 7). The increase and normal values of the Th/U ratio recorded in these first meters of the succession support the fact that the Microcodium Formation was deposited in marine and continental environments within a supratidal setting under low energy conditions (Figs. 4 and 6). The lack of any other fossil content in the Microcodium Formation, except for some unlined meniscate burrows (*Taenidium*), is characteristic of the base of this formation, confirming its proximal character (e.g., Arena et al., 2024).

The optimal conditions to develop the *Microcodium* are in a semi-arid or dry climate, and tropical and semi-tropical environments (e.g., Murru et al., 2003; Molina et al., 2006; Molina and Nieto, 2008; Kabanov et al., 2010). As discussed above, the Th/K ratio indicates that smectite prevailed in this part of the stratigraphic succession, probably favored by semi-arid/or dry conditions that reigned during the pre-Bartonian (Paleocene? or early Eocene?).

The deposition of the Capo Mortola Calcarenite Formation marks the beginning of a marine transgression that represents the earliest sedimentation during the onset of subsidence around the Alpine Arc, reflecting the effects of both tectonics and eustasy (Sayer, 1995; Sinclair et al., 1998; Varrone and Clari, 2003). In the Olivetta SM section, the initial marine transgression represents a transition from subaerially land to shallow marine deposits until reaching the deepening of the ramp, as recorded by the LFs together with the fossil content through the Bartonian (Fig. 7). The normal marine conditions of this formation are supported by values of the Th/U ratio and by carbonate deposition (limestone) developed in the basin dominated by larger benthic foraminifera (LBF) and other calcareous fossils (e.g., Arena et al., 2024).

The Capo Mortola Calcarenite Formation shows an overall deepening from base to top, possibly controlled by subsidence. However, the cyclicity within the stratigraphic succession represents cycles of progradation of the carbonate ramp out into the basin, suggesting that the productivity of the carbonate system was able to match or even outpace the creation of accommodation space during the early stages of transgression. The upper part of the Capo Mortola Calcarenite Formation is marked by a cyclicity dominated by deepening upward facies. This cyclicity is thought to be due to the increased effects of subsidence on the relative sea level, producing the transition to the Olivetta San Michele Silty-Marl Formation (Figs. 5 and 7).

The paleobathymetry of the carbonate ramp is closely linked to marine transgression and its deepening, as evidenced by the evolution of the fossil content, since habitats can be delimited in shallow subtidal waters. The fauna dominating lower cycle II in the Olivetta SM section that corresponds to the LF2 is composed of LBF, bivalves, gastropods, and corals that inhabited seafloors shallower than 30 m and were deposited in a regime of moderate energy (Arena et al., 2024) (Fig. 7). Moreover, cycle III is characterized by taxa like the previous ones and some diverse LBF, followed by a short period barren of fossils, which is interpreted between 30 and 50 m deep in a low-energy regime (Arena et al., 2024) (Fig. 7). Cycle IV is marked by an increase in orthophragmines, *Operculina*, and planktonic foraminifera, with an inferred depth >50 m, again in a low-energy regime (Gandolfi et al., 2023; Arena et al., 2024) (Fig. 7)..

The evolution of the drowning carbonate ramp in the Olivetta SM section is interpreted to be the result of several factors that were dominated by a rapid subsidence of the basin and an increase in nutrients. The latter probably reduced the productivity of the carbonate ramp due to the renewal of terrigenous input into the distal part of the basin (Hallock and Schlager, 1986; Sayer, 1995). The top of the Capo Mortola Calcarenite Formation is marked by the drowning of the ramp and the rapid transition to the Olivetta San Michele Silty-Marl Formation, evidenced by a maximum flooding surface characterized by reworked bioclasts and abundant authigenic minerals, which suggest the demise of the carbonate factory (Sayer, 1995; Sinclair et al., 1998; Allen et al., 2001; Varrone and Clari, 2003; Varrone and d'Atri, 2007).

6. Conclusions

This study provides a detailed description and interpretation of the paleoenvironmental conditions of a mixed carbonate-siliciclastic ramp cropping out in the vicinity of the village of Olivetta San Michele in the southern Provençal Domain. The succession records the early underfilled foreland basin of the Ligurian Alps, represented by the Microcodium Formation and the Capo Mortola Calcarenite Formation.

SGR, used as a proxy for the paleoclimatic reconstruction and the identification of depositional cycles, together with previously published data on the lithological description of the fossil content, allow us to propose a new paleoenvironmental reconstruction of the Olivetta SM section. The degree of correlation between the paleoclimate and paleoenvironmental-sensitive indicators is analyzed by means of the Th/K and Th/U ratios, giving an interpretation of the changes in the studied Paleogene section. Low Th/U ratios are associated with marine normal conditions, whereas high Th/U ratios are related to continental environments. In turn, high Th/K ratios are linked with clay-mineral suites dominated by kaolinite and/or smectite, whereas low Th/K ratios are associated with clay-mineral assemblages dominated by illite.

The Microcodium Formation records a combination of high and low Th/U ratios, indicating transitional marine-continental conditions. This is confirmed by the recorded lithofacies and *Microcodium* grains, which are interpreted as deposits of subaerial, shallow-marine, and estuarine origin, developed in a supratidal environment prior to marine transgression. The values of the Th/K ratio suggest that smectite was the dominant clay mineral, which is associated with a semi-arid climate.

The Capo Mortola Calcarenite Formation presents low Th/U ratios typical of marine oxic-normal environments, characterized by their lithofacies and fossil content, indicating the beginning of the transgression and the deepening of the carbonate-siliciclastic ramp in a subtidal environment. High Th/K ratios permit the identification of typical values for kaolinite and smectite, which are alternating throughout the whole section. This alternation may be indicative of climatic fluctuations, where kaolinite reflects humid conditions during long dry periods, whereas the dominant smectite may be controlled by regional changes in a warm-humid climate and wet-dry seasonal alternations, as evidenced in the Mediterranean basins during the Paleocene

and Eocene.

The information gained from the SGR trends corresponds to changes in grain size, clay content, and mineralogy. These log trends may be calibrated to stacking patterns that indicate progradational, retrogradational, and aggradational cycles, representing depositional systems that vary through time and space. The short cycles are reconstructed by the signal of the SGR, and the long cycles are derived from a novel log-based approach called derivative trend analysis (DTA), which prepares the mathematical signal of the SGR in a final new curve of the SGR that delimits regressive and transgressive cycles. Most of the short cycles in the Olivetta SM section are characteristic of coarsening upward patterns. The Microcodium Formation (short cycles: 4 coarsening upward and 1 fining upward) is characterized by one long cycle that corresponds to a regression. The Capo Mortola Calcarenite Formation (short cycles: 7 coarsening upward and 5 shallowing upward) is characterized by three long cycles (transgressive-regressive) that are associated with the marine transgression during the Eocene in the French-Italian Maritime Alps (Dauphinois-Provençal domain) and on the France-Switzerland border.

CRediT authorship contribution statement

Victor M. Giraldo-Gómez: Writing – review & editing, Writing – original draft, Methodology, Investigation, Data curation, Conceptualization. **Michele Piazza:** Writing – review & editing, Writing – original draft, Methodology, Investigation, Funding acquisition, Conceptualization. **Luca Arena:** Writing – original draft, Methodology, Data curation. **Andrea Baucon:** Writing – review & editing, Writing – original draft, Data curation. **Antonella Gandolfi:** Writing – review & editing, Writing – original draft, Methodology, Data curation. **Cesare A. Papazzoni:** Writing – review & editing, Writing – original draft, Methodology. **Johannes Pignatti:** Writing – review & editing, Writing – original draft, Methodology, Investigation, Data curation. **Antonino Briguglio:** Writing – review & editing, Writing – original draft, Project administration, Methodology, Investigation, Funding acquisition, Data curation, Conceptualization.

Declaration of competing interest

The authors declare that they have no known competing financial interests or personal relationships that could have appeared to influence the work reported in this paper.

Data availability

Data will be made available on request.

Acknowledgments

This study was supported by the University of Genova, which funded the Curiosity Driven Project awarded to AB on Ligurian Palaeoenvironments, and the Ministry of Education, University and Research (MIUR), Italy, which funded the PRIN 2017 “Biota resilience to global change: biomineralization of planktic and benthic calcifiers in the past, present and future” (prot.2017RX9XXY). MP thanks FRA 2022 University of Genova for the support of this project. We thank Wolfgang Eder (formerly at the University of Genova), Sulia Goeting (University of Lausanne), and Eleni Lutaj (University of Genova) for their help in the field.

Appendix A. Supplementary data

Supplementary data to this article can be found online at https://doi.org/10.1016/j.marpetgeo.2024.106752.

References

Adams, J.A., Weaver, C.E., 1958. Thorium-to-Uranium ratios as indicators of sedimentary processes: example of concept of geochemical facies. AAPG Bull. 42 (2), 387–430.

Allen, P.A., Crampton, S.L., Sinclair, H.D., 1991. The inception and early evolution of the North Alpine foreland basin, Switzerland. Basin Res. 3 (3), 143–163.

Allen, P.A., Burgess, P.M., Galewsky, J., Sinclair, H.D., 2001. Flexural-eustatic numerical model for drowning of the Eocene perialpine carbonate ramp and implications for Alpine geodynamics. Geol. Soc. Am. Bull. 113 (8), 1052–1066.

Arena, L., Giraldo-Gómez, V.M., Baucon, A., Piazza, M., Papazzoni, C.A., Pignatti, J., Gandolfi, A., Briguglio, A., 2024. Short-term middle Eocene (Bartonian) paleoenvironmental changes in the sedimentary succession of Olivetta San Michele (NW Italy): the response of shallow-water biota to climate in NW Tethys. Facies 70 (4), 259–284. https://doi.org/10.1007/s10347-023-00677-4.

Apps, G., Peel, F., Elliott, T., 2004. The structural setting and palaeogeographical evolution of the Grès d’Annot basin. Geol. Soc. Spec. Publ. 221 (1), 65–96. https://doi.org/10.1144/GSL.SP.2004.221.01.05.

Basu, H., Mahendra Kumar, K., Paneerselvam, S., Chaki, A., 2009. Study of provenance characteristics and depositional history on the basis of U, Th and K abundances in the Gulcheru formation, Cuddapah basin in Tummalapalle–Somalollapalle areas, Cuddapah-Anantapur Districts, Andhra Pradesh. J. Geol. Soc. India 74 (3), 318–328. https://doi.org/10.1007/s12594-009-0136-3.

Bendias, D., Aigner, T., 2015. Facies, sequence stratigraphy, reservoir and seal potential of the Mafraq Formation, Sultanate of Oman: an integrated outcrop analogue study. GeoArabia 20 (3), 17–94.

Bessa, J., 1995. High-resolution Outcrop Gamma-Ray Spectrometry of the Lower Lias, Southern Britain. Doctoral Dissertation (PhD). University of Oxford, Oxford, UK, p. 247.

Bessa, J.L., Hesselbo, S.P., 1997. Gamma-ray character and correlation of the Lower Lias, SW Britain. Proc. Geol. Assoc. 108 (2), 113–129.

Bolle, M.P., Adatte, T., 2001. Palaeocene-early Eocene climatic evolution in the Tethyan realm: clay mineral evidence. Clay Miner. 36 (2), 249–261.

Boussac, J., 1912. Études stratigraphiques sur le Nummulitique alpin. Mém. Serv. Carte Géol. Paris, France, p. 662.

Brandano, M., 2019. The role of oceanographic conditions on Cenozoic carbonate platform drowning: insights from Alpine and Apennine foreland basins. Terra Nova. 31 (2), 102–110.

Briguglio, A., Giraldo-Gomez, V.M., Baucon, A., Benedetti, A., Papazzoni, C.A., Pignatti, J., Wolfgring, E., Piazza, M., 2024. Depositional environments in incipient drowning ramps: insights from a Bartonian shallow water sedimentary succession in NW Italy. Newsl. Stratigr. 5 (1), 37–63. https://doi.org/10.1127/nos/2023/0784.

Campredon, R., 1977. Les formations paléogènes des Alpes Maritimes franco-italiennes. Mém. h. sér. Soc. géol. France. 9, 1–199.

Campredon, R., Giannerini, G., 1982. Le synclinal de Saint-Antonin (arc de Castellane, chaînes subalpines méridionales) Un exemple de bassin soumis à une déformation compressive permanente depuis l’Eocène supérieur. Geol. Alpine 58, 15–20.

Cao, L., Zhang, Z., Zhao, J., Jin, X., Li, H., Li, J., Wei, X., 2021. Discussion on the applicability of Th/U ratio for evaluating the paleoredox conditions of lacustrine basins. Int. J. Coal Geol. 248, 1–17. https://doi.org/10.1016/j.coal.2021.103868.

Castelltort, S., Guillocheau, F., Robin, C., Rouby, D., Nalpas, T., Lafont, F., Eschard, R., 2003. Fold control on the stratigraphic record: a quantified sequence stratigraphic study of the Pico del Aguila anticline in the south-western Pyrenees (Spain). Basin Res. 15, 527–551. https://doi.org/10.1046/j.1365-2117.2003.00218.x.

Catuneanu, O., 2019. Scale in sequence stratigraphy. Mar. Petrol. Geol. 106, 128–159.

Catuneanu, O., 2022. Principles of Sequence Stratigraphy, second ed. Elsevier Science, p. 486.

Chamley, H., 1989. Clay Formation through weathering. In: Clay Sedimentology. Springer, Berlin, Heidelberg, pp. 21–50. https://doi.org/10.1007/978-3-642-85916-8_2.

Chamley, H., 2001. Clay mineralogy. In: Encyclopedia of Ocean Science, first ed. Academic Press, pp. 462–471.

Chiarella, D., Longhitano, S.G., Tropeano, M., 2017. Types of mixing and heterogeneities in siliciclastic-carbonate sediments. Mar. Petrol. Geol. 88, 617–627.

Coletti, G., Mariani, L., Garzanti, E., Consani, S., Bosio, G., Vezzoli, G., Hu, X., Basso, D., 2021. Skeletal assemblages and terrigenous input in the Eocene carbonate systems of the Nummulitic Limestone (NW Europe). Sediment. Geol. 425, 1–23. https://doi.org/10.1016/j.sedgeo.2021.106005.

Crevello, P.D., Franseen, E.K., Watney, W.L., 1991. High-frequency carbonate cycles and stacking patterns: interplay of orbital forcing and subsidence on lower Jurassic rift platforms, high Atlas, Morocco. Sedimentary modeling: computer Simulations and methods for Improved Parameter definition. KGS. Bull. 233, 207–230.

Cowan, D.R., Myers, K.J., 1988. Surface gamma ray logs: a correlation tool for frontier areas. AAPG Bull. 72, 634–636.

Dallagiovanna, G., Fanucci, F., Pellegrini, L., Seno, S., Bonini, L., Decarlis, A., Maino, M., Morelli, D., Toscani, G., con contributi di Breda, A., Vercesi, P.L., Zizioli, D., Cobianchi, M., Mancin, N., Papazzoni, C.A., 2012a. Note Illustrative Della Carta Geologica Foglio 257 - Dolceacqua Regione Liguria, p. 75. http://www.cartografia.regione.liguria.it/templateFogliaRC.asp.

Dallagiovanna, G., Fanucci, F., Pellegrini, L., Seno, S., Decarlis, A., Maino, M., Toscani, G., 2012b. Carta Geologica alla scala 1: 25000 Foglio 257 “Dolceacqua” e Foglio 270 “Ventimiglia” con note ilustrative. Regione Liguria.

Day-Stirrat, R.J., Hillier, S., Nikitin, A., Hofmann, R., Mahood, R., Mertens, G., 2021. Natural gamma-ray spectroscopy (NGS) as a proxy for the distribution of clay minerals and bitumen in the Cretaceous McMurray Formation, Alberta, Canada. Fuel 288, 119513. https://doi.org/10.1016/j.fuel.2020.119513.

de Graciansky, P.C., Roberts, D.G., Tricart, P., 2010. The Western Alps, from Rift to Passive Margin to Orogenic Belt: an Integrated Geoscience Overview. Elsevier, p. 432.
Decarlis, A., Maino, M., Dallagiovanna, G., Lualdi, A., Masini, E., Seno, S., Toscani, G., 2014. Salt tectonics in the SW Alps (Italy–France): from rifting to the inversion of the European continental margin in a context of oblique convergence. Tectonophysics 636, 293–314.
Deconinck, J.-F., 1992. Sédimentologie des argiles dans le Jurassique-Crétacé d'Europe occidentale et du Maroc. Doctoral dissertation. Université des Sciences et Technologie de Lille. Lille, France 106.
Deconinck, J.-F., Hesselbo, S.P., Debuisser, N., Averbuch, O., Baudin, F., Bessa, J., 2003. Environmental controls on clay mineralogy of an early Jurassic mudrock (blue Lias formation, southern England). Int. J. Earth Sci. 92 (2), 255–266. https://doi.org/10.1007/s00531-003-0318-y.
Di Capua, A., Barilaro, F., Groppelli, G., 2021. Volcanism and volcanogenic submarine sedimentation in the Paleogene Foreland Basins of the Alps: reassessing the source-to-sink systems with an actualist view. Geosciences 11 (1), 23. https://doi.org/10.3390/geosciences11010023.
Diester-Haass, L., Robert, C., Chamley, H., 1998. Paleoproductivity and climate variations during sapropel deposition in the eastern Mediterranean Sea. Proc. Ocean Drill. Prog., Sci. results. 160, 227–248.
Doveton, J.H., 1994. Geologic log analysis using computer methods. AAPG Bull. 169.
Dunham, R.J., 1962. In: Ham, W.E. (Ed.), Classification of Carbonate Rocks According to Depositional Texture. AAPG Memoir, Tulsa, pp. 108–121.
Dypvik, H., Harris, N.B., 2001. Geochemical facies analysis of fine-grained siliciclastics using Th/U, Zr/Rb and (Zr+Rb)/Sr ratios. Chem. Geol. 181 (1–4), 131–146. https://doi.org/10.1016/S0009-2541(01)00278-9.
Ehrenberg, S.N., Svana, T.A., Swart, P.K., 2008. Uranium depletion across the Permian–Triassic boundary in Middle East carbonates: Signature of oceanic anoxia. AAPG Bull. 92 (6), 691–707. https://doi.org/10.1306/02140807095.
Ellis, D.V., Singer, J.M., 2007. Well Logging for Earth Scientists, Second ed. Springer, p. 728.
Fabricius, I.L., Fazladic, L.D., Steinholm, A., Korsbech, U., 2003. The use of spectral natural gamma-ray analysis in reservoir evaluation of siliciclastic sediments: a case study from the Middle Jurassic of the Harald Field, Danish Central Graben. Geol. Surv. Den. Greenl. Bull. 1, 349–366.
Ferràndez-Cañadell, C., Baumgartner-Mora, C., Baumgartner, P.O., Epard, J.L., 2023. Priabonian (upper Eocene) larger foraminifera from the Helvetic Nappes of the alps (western Switzerland): new markers for shallow benthic zones 19–20. Micropaleontology 69 (4), 401–449.
Flügel, E., 2012. Microfacies of Carbonate Rocks: Analysis. Interpretation and Springer Science & Business Media, Berlin, p. 984.
Ford, M., Duchene, S., Gasquet, D., Vanderhaeghe, O., 2006. Two-phases orogenic convergence in the external and internal Alps. J. Geol. Soc. London. 163, 815–826.
Gandolfi, A., Giraldo-Gómez, V.M., Luciani, V., Piazza, M., Adatte, T., Arena, L., Bomou, B., Fornaciari, E., Frijia, G., Kocsis, L., Briguglio, A., 2023. The Middle Eocene Climatic Optimum (MECO) impact on the benthic and planktic foraminiferal resilience from a shallow-water sedimentary record. Riv. Ital. Paleontol. 129 (3), 629–651.
Gao, Y., Xi, D., Qin, Z., Ma, P., Wang, C., 2018. Clay mineralogy of the first and second members of the Nenjiang Formation, Songliao basin: implications for paleoenvironment in the Late Cretaceous. Science China. Earth Sci. 61 (3), 327–338. https://doi.org/10.1007/s11430-017-9110-9.
Gèze, B., Lanteaume, M., Peyre, Y., Vernet, J., Nesteroff, W., 1968. Carte géologique de la France au 1: 50.000, Feuille Menton-Nice, XXXVII-42 et 43. B.R.G.M. Orléans, p. 17.
Giammarino, S., Orezzi, S., Piazza, M., Rosti, D., 2009. Evidence of syn-sedimentary tectonic activity in the "flysch di Ventimiglia" (Ligurian Alps foredeep basin). Ital. J. Geosci. 128 (2), 467–472. https://doi.org/10.3301/IJG.2009.128.2.467.
Gèze, B., Nestéroff, W., 1996. Notice explicative, carte géol. France (1/50 000). In: Feuille Menton-Nice. XXXVII-42-43. B.R.G.M. Orléans, p. 17.
Giammarino, S., Fanucci, F., Orezzi, S., Rosti, D., Morelli, D., Cobianchi, M., De Stefanis, A., Di Stefano, A., Finocchiaro, F., Fraveg, a P., Piazza, M., Vannucci, G., 2010. Note Illustrative Della Carta Geologica d'Italia Alla Scala 1:50.000 - Foglio San Remo N. 258–271. ISPRA – Regione Liguria, p. 130.
Giorgioni, M., Jovane, L., Rego, E.S., Rodelli, D., Frontalini, F., Coccioni, R., Catanzariti, R., Özcan, E., 2019. Carbon cycle instability and orbital forcing during the middle Eocene climatic optimum. Sci. Rep. 9, 1–10. https://doi.org/10.1038/s41598-019-45763-2.
Glover, P.W., 2000. Petrophysics. University of Aberdeen, UK, p. 270.
Grabau, A.W., 1904. American Geologist. In: On the Classification of Sedimentary Rocks. Princeton University, p. 247.
Gupta, S., Allen, P.A., 1999. Fossil shore platforms and drowned gravel beaches: evidence for high frequency sea-level fluctuations in the distal Alpine foreland basin. J. Sediment. Res. 69, 394–413.
Hallock, P., Schlager, W., 1986. Nutrient excess and the demise of coral reefs and carbonate platforms. Palaios 1, 389–398.
Hammer, Ø., Harper, D.A., Ryan, P.D., 2001. PAST: Paleontological statistics software package for education and data analysis. Palaeontol. Electron. 4 (1), 9.
Handy, M.R., Schmid, S.M., Bousquet, R., Kissling, E., Bernoulli, D., 2010. Reconciling plate-tectonic reconstructions of Alpine Tethys with the geological–geophysical record of spreading and subduction in the Alps. Earth Sci. Rev. 102 (3–4), 121–158.
Haq, B.U., Hardenbol, J.A.N., Vail, P.R., 1987. Chronology of fluctuating sea levels since the Triassic. Science 235 (4793), 1156–1167.
Henglai, P., 2018. Sequence-stratigraphic and facies controls on reservoir quality and productivity of Early to Middle Miocene fluvial and tide-dominated deltaic deposits, Formation 2, Gulf of Thailand. Master Thesis. University of Oklahoma, USA 138.
Hesselbo, S.P., Morgans-Bell, H.S., McElwain, J.C., Rees, P.M., Robinson, S.A., Ross, C.E., 2003. Carbon-cycle perturbation in the Middle Jurassic and accompanying changes in the terrestrial paleoenvironment. Geol. J. 111 (3), 259–276.
Hesselbo, S.P., Deconinck, J.-F., Huggett, J.M., Morgans-Bell, H.S., 2009. Late Jurassic palaeoclimatic change from clay mineralogy and gamma-ray spectrometry of the Kimmeridge Clay, Dorset, UK. J Geol Soc London 166 (6), 1123–1133.
Homewood, P., Mauriaud, P., Lafont, F., 2000. Best practices in sequence stratigraphy: for explorationists and reservoir engineers. Elf EP mem 25, 81.
Honegger, L., Adatte, T., Spangenberg, J.E., Rugenstein, J.K.C., Poyatos-Moré, M., Puigdefàbregas, C., Castelltort, S., 2020. Alluvial record of an early Eocene hyperthermal within the Castissent formation, the Pyrenees, Spain. Clim. Past. 16 (1), 227–243.
Kabanov, P., Anadón, P., Krumbein, W.E., 2008. Microcodium: an extensive review and a proposed non-rhizogenic biologically induced origin for its formation. Sediment. Geol. 205 (3–4), 79–99.
Kabanov, P.B., Alekseeva, T.V., Alekseeva, V.A., Alekseev, A.O., Gubin, S.V., 2010. Paleosols in late Moscovian (Carboniferous) marine carbonates of the East European craton revealing "great calcimagnesian plain" paleolandscapes. J. Sediment. Res. 80 (3), 195–215.
Kennedy, M.J., Wagner, T., 2011. Clay mineral continental amplifier for marine carbon sequestration in a greenhouse ocean. Proc. Natl. Acad. Sci. USA 108 (24), 9776–9781. https://doi.org/10.1073/pnas.1018670108.
Krassay, A.A., 1998. Outcrop and drill core gamma-ray logging integrated with sequence stratigraphy: examples from Proterozoic sedimentary successions of northern Australia. AGSO J. Aust. Geol. Geophys. 17, 285–300.
Kouamelan, K.S., Zou, C., Wang, C., Assie, K.R., Peng, C., Mondah, O.R., Brantson, E.T., 2020. Multifractal characterization of the Coniacian–Santonian OAE3 in lacustrine and marine deposits based on spectral gamma ray logs. Sci. Rep. 10 (1), 1–22. https://doi.org/10.1038/s41598-020-71327-w.
Lanteaume, M., 1968. Contribution à l'étude géologique des Alpes Maritimes franco-italiennes. Mém. serv. Carte Géol. France. 1–405.
Lehrmann, D.J., Goldhammer, R.K., 1999. Secular variation in parasequence and facies stacking patterns of platform carbonates: a guide to application of stacking-patterns analysis in strata of diverse ages and settings. SEPM (Soc. Sediment. Geol.) Spec. Publ. 63, 421.
Lemoine, M., Bas, T., Arnaud-Vanneau, A., Arnaud, H., Dumont, T., Gidon, M., Bourbon, M., de Graciansky, P.C., Rudkiewicz, J.L., Megard-Galli, J., Tricart, P., 1986. The continental margin of the Mesozoic Tethys in the western Alps. Mar. Petrol. Geol. 3 (3), 179–199. https://doi.org/10.1016/0264-8172(86)90044-9.
Li, X., Wang, D., Liu, Q., Komarneni, S., 2019. A comparative study of synthetic tubular kaolinite nanoscrolls and natural halloysite nanotubes. Appl. Clay Sci. 168, 421–427.
Luthi, S., 2001. Geological Well Logs: Their Use in Reservoir Modeling. Springer Science & Business Media. Springer-Verlag Berlin Heidelberg, p. 373. https://doi.org/10.1007/978-3-662-04627-2.
Longhitano, S.G., Sabato, L., Tropeano, M., Gallicchio, S., 2010. A mixed bioclastic–siliciclastic flood-tidal delta in a micro tidal setting: depositional architectures and hierarchical internal organization (Pliocene, Southern Apennine, Italy). J. Sediment. Res. 80 (1), 36–53.
Maino, M., Seno, S., 2016. The thrust zone of the Ligurian Penninic basal contact (Monte Fronté, Ligurian alps, Italy). J. Maps 12 (1), 341–351. https://doi.org/10.1080/17445647.2016.1213669.
Marini, M., Patacci, M., Felletti, F., Decarlis, A., McCaffrey, W., 2022. The erosionally confined to emergent transition in a slope-derived blocky mass-transport deposit interacting with a turbidite substrate, Ventimiglia Flysch Formation (Grès d'Annot System, north-west Italy). Sedimentology 69 (4), 1675–1704.
Martín-Martín, M., Rey, J., Alcala-Garcia, F.J., Tosquella, J., Deramond, J., Lara-Corona, E., Antoine, P.O., 2001. Tectonic controls on the deposits of a foreland basin: an example from the Eocene Corbières–Minervois basin. France. Basin Res. 13 (4), 419–433.
Martín-Martín, M., Guerrera, F., Tosquella, J., Tramontana, M., 2021. Middle Eocene carbonate platforms of the westernmost Tethys. Sediment. Geol. 415, 105861.
Martín-Martín, M., Tosquella, J., Guerrera, F., Maaté, A., Hlila, R., Maaté, S., Le Breton, E., 2023. The Eocene carbonate platforms of the Ghomaride domain (internal Rif zone, N Morocco): a segment of the westernmost Tethys. Sediment. Geol. 452, 106423 https://doi.org/10.1016/j.sedgeo.2023.106423.
McKinley, J., Lloyd, C., Ruffell, A., 2003. Macro-to micro-scale controls on reservoir properties of the Sherwood Sandstone group of north-east Ireland. Ir. J. Earth Sci. 21, 143–165.
Mernagh, T.P., Miezitis, Y., 2008. A Review of the Geochemical Processes Controlling the Distribution of Thorium in the Earth's Crust and Australia's Thorium Resources. Geoscience Australia, Canberra, Australia, p. 57.
Messaoud, J.H., Thibault, N., Bomou, B., Adatte, T., Monkenbusch, J., Spangenberg, J.E., Yaich, C., 2021. Integrated stratigraphy of the middle-upper Eocene souar formation (Tunisian dorsal): implications for the middle Eocene climatic optimum (MECO) in the SW Neo-Tethys. Palaeogeogr. Palaeoclimatol. Palaeoecol. 581, 1–18. https://doi.org/10.1016/j.palaeo.2021.110639.
Molina, J.M., Vera, J.A., Aguado, R., 2006. Reworked Microcodium calcarenites interbedded in pelagic sedimentary rocks (Paleocene, Subbetic, southern Spain): paleoenvironmental reconstruction. In: Alonso-Zarza, A.M., Tanner, L.H. (Eds.), Paleoenvironmental record and applications of calcretes and palustrine carbonates. Geol. Soc. Am. Spec. Pap. 416, pp. 189–202. https://doi.org/10.1130/2006.2416(12.
Molina, J.M., Nieto, L.M., 2008. Microcodium en calizas del Eoceno Medio (Luteciense) de la Sierra de la Pila (Prebético Interno, Murcia). Geogaceta 44, 111–114.
Morelli, D., Locatelli, M., Corradi, N., Cianfarra, P., Crispini, L., Federico, L., Migeon, S., 2022. Morpho-structural setting of the Ligurian Sea: the role of structural heritage

and neotectonic inversion. J. Mar. Sci. Eng. 10 (9), 1–24. https://doi.org/10.3390/jmse10091176.
Mount, J.F., 1984. Mixing of siliciclastic and carbonate sediments in shallow shelf environments. Geology 12 (7), 432–435.
Mueller, P., Maino, M., Seno, S., 2020. Progressive deformation patterns from an accretionary prism (Helminthoid flysch, Ligurian alps, Italy). Geosciences 10 (26), 1–17. https://doi.org/10.3390/geosciences10010026.
Murru, M., Ferrara, C., Da Pelo, S., Ibba, A., 2003. The Palaeocene–Middle Eocene deposits of Sardinia (Italy) and their palaeoclimatic significance. CR Geosci 335 (2), 227–238.
Myers, K.J., 1987. Onshore Outcrop Gamma Ray Spectrometry as a Tool in Sedimentological Studies. PhD Thesis. University of London, London, UK, p. 310.
Myers, K.J., Wignall, P.B., 1987. Understanding Jurassic organic-rich mudrocks–new concepts using gamma-ray spectrometry and palaeoecology: examples from the Kimmeridge Clay of Dorset and the Jet Rock of Yorkshire. In: Leggett, J.K., Zuffa, G. G. (Eds.), Marine Clastic Sedimentology: Concepts and Case Studies. Springer, 172–189.
Paredes, J.M., Giordano, S.R., Olazábal, S.X., Valle, M.N., Allard, J.O., Foix, N., Tunik, M. A., 2020. Climatic control on stacking and connectivity of fluvial successions: upper Cretaceous Bajo barreal formation of the Golfo san Jorge basin, Patagonia. Mar. Petrol. Geol. 113, 104116 https://doi.org/10.1016/j.marpetgeo.2019.104116.
Peris Cabré, S., Valero, L., Spangenberg, J.E., Vinyoles, A., Verité, J., Adatte, T., Maxime Tremblin, M., Watkins, S., Sharma, N., Garcés, M., Puigdefàbregas, C., Castelltort, S., 2023. Fluvio-deltaic record of increased sediment transport during the middle Eocene climatic optimum (MECO), southern Pyrenees, Spain. Clim. Past. 19 (3), 533–554. https://doi.org/10.5194/cp-19-533-2023.
Perotti, E., Bertok, C., d'Atri, A., Martire, L., Piana, F., Catanzariti, R., 2012. A tectonically-induced Eocene sedimentary mélange in the west Ligurian Alps Italy. Tectonophysics 568, 200–214. https://doi.org/10.1016/j.tecto.2011.09.005.
Peterhänsel, A., Egenhoff, S.O., 2008. Lateral variabilities of cycle stacking patterns in the Latemar, Triassic, Italian Dolomites. In: Controls on Carbonate Platform and Reef Development, vol. 89. SEPM Spec. Publ, pp. 17–229. https://doi.org/10.2110/pec.08.89.0217.
Quirein, J.A., Gardner, J.S., Watson, J.T., 1982. Combined natural gamma ray spectral/litho-density measurements applied to complex lithologies. In: SPE Annual Technical Conference and Exhibition. SPE, vol. 11143, pp. 1–4.
Reolid, M., Iwańczuk, J., Mattioli, E., Abad, I., 2020. Integration of gamma ray spectrometry, magnetic susceptibility and calcareous nannofossils for interpreting environmental perturbations: an example from the Jenkyns Event (lower Toarcian) from South Iberian Palaeomargin (Median Subbetic, SE Spain). Palaeogeogr. Palaeoclimatol. Palaeoecol. 560, 110031 https://doi.org/10.1016/j.palaeo.2020.110031.
Reuter, M., Piller, W.E., Brandano, M., Harzhauser, M., 2013. Correlating Mediterranean shallow-water deposits with global Oligocene–Miocene stratigraphy and oceanic events. Global Planet. Change 111, 226–236. https://doi.org/10.1016/j.gloplacha.2013.09.018.
Robert, H., Chamley, H., 1991. Development of Early Eocene warm climates, as inferred from clay mineral variations in oceanic sediments. Palaeogeogr. Palaeoclimatol. Palaeoecol. 89 (4), 315–331. https://doi.org/10.1016/0031-0182(91)90169-R.
Rodríguez-Tovar, F.J., Pujalte, V., Payros, A., 2020. Danian-lower Selandian Microcodium-rich calcarenites of the Subbetic zone (SE Spain): record of Nereites ichnofacies in a deep-sea, base-of-slope system. Sediment. Geol. 406, 105723.
Ruffell, A., Worden, R., 2000. Palaeoclimate analysis using spectral gamma-ray data from the Aptian (Cretaceous) of southern England and southern France. Palaeogeogr. Palaeoclimatol. Palaeoecol. 155 (3–4), 265–283. https://doi.org/10.1016/S0031-0182(99)00119-4.
Ruffell, A., McKinley, J.M., Lloyd, C.D., Graham, C., 2006. Th/K and Th/U ratios from spectral gamma-ray surveys improve the mapped definition of subsurface structures. J. Environ. Eng. Geophys. 11 (1), 53–61.
Ruffell, A., Kürschner, W.M., 2020. Sediment cyclicity and the Carnian Pluvial Episode: evidence from spectral gamma ray logging of the Mercia mudstone group, SW England. Bol. Geol. Min. 131 (2), 231–242. https://doi.org/10.21701/bolgeomin.131.2.002.
Sayer, Z.R., 1995. The Nummulitique: carbonate deposition in a foreland basin setting; Eocene, French alps. PhD Thesis. Durham University. Durham, UK 351. http://etheses.dur.ac.uk/6103/.
Scheibner, C., Speijer, R.P., 2008. Late Paleocene–early Eocene Tethyan carbonate platform evolution—a response to long-and short-term paleoclimatic change. Earth Sci. Res. 90 (3–4), 71–102.
Schlumberger, 1997. Log Interpretation Charts. Schlumberger Wireline & Testing. Schlumberger Ltd, Houston, Texas, USA, p. 193.
Schnyder, J., Ruffell, A., Deconinck, J.-F., Baudin, F., 2006. Conjunctive use of spectral gamma-ray logs and clay mineralogy in defining late Jurassic–early Cretaceous palaeoclimate change (Dorset, UK). Palaeogeogr. Palaeoclimatol. Palaeoecol. 229 (4), 303–320.
Seno, S., Fanucci, F., Dallagiovanna, G., Maino, M., Pellegrini, L., Vercesi, P.L., Morelli, D., Savini, A., Migeon, S., Cobianchi, M., Mancin, N., Marini, M., Felletti, F., Decarlis, A., Maino, M., Toscani, G., Breda, A., Zizioli, D., 2012. Carta Geologica alla scala 1:50000 Foglio 257. "Dolceacqua" e Foglio 270 "Ventimiglia". https://www.isprambiente.gov.it/Media/carg/257_270_DOLCEACQUA_VENTIMIGLIA/Foglio.
Serra-Kiel, J., Travé, A., Mató, E., Saula, E., Ferràndez-Cañadell, C., Busquets, P., Tosquella, J., Vergés, J., 2003. Marine and transitional Middle/Upper Eocene units of the southeastern Pyrenean foreland basin (NE Spain). Geol. Acta 1 (2), 177–200.
Sinclair, H.D., 1997. Tectonostratigraphic model for underfilled peripheral foreland basins: an Alpine perspective. Geol. Soc. Am. Bull. 109 (3), 324–346. https://doi.org/10.1130/0016-7606(1997)109<0324:TMFUPF>2.3.CO;2.
Sinclair, H.D., Sayer, Z.R., Tucker, M.E., 1998. Carbonate sedimentation during early foreland basin subsidence: the Eocene succession of the French Alps. Geol. Soc. Spec. Publ. 149 (1), 205–227.
Slatt, R.M., Jordan, D.W., D'Agostino, A.E., Gillespie, R.H., 1992. Outcrop gamma-ray logging to improve understanding of subsurface well log correlations. Geol. Soc. Spec. Publ. 65 (1), 3–19.
Spofforth, D.J.A., Agnini, C., Pälike, H., Rio, D., Fornaciari, E., Giusberti, L., Luciani, V., Lanci, L., Muttoni, G., 2010. Organic carbon burial following the middle Eocene climatic optimum in the central western Tethys. Paleoceanography 25 (3), 1–11.
Varrone, D., 2004. Le prime fasi di evoluzione del bacino di avanfossa alpino: la successione Delfinese cretacico-eocenica, Alpi Marittime. Tesi di Dottorato, Dip. Scienze della Terra, Università degli Studi di Torino, Torino, Italia, p. 145pp.
Varrone, D., Clari, P., 2003. Évolution stratigraphique et paléoenvironnementale de la Formation à Microcodium et des Calcaires à Nummulites dans les Alpes Maritimes franco-italiennes. Geobios 36, 775–786. https://doi.org/10.1016/j.geobios.2003.09.001.
Varrone, D., d'Atri, A., 2007. Acervulinid macroid and rhodolith facies in the Eocene Nummulitic limestone of the Dauphinois domain (Maritime alps, Liguria, Italy). Swiss J. Geosci. 100 (3), 503–515.
Varrone, D., Decrouez, D., 2007. Eocene larger foraminiferal biostratigraphy in the southernmost Dauphinois Domain (Maritime Alps, France-Italy border). Riv. Ital. Paleontol. Stratigr. 113 (2), 257–267.
Vail, P.R., Mitchum Jr., R.M., Thompson III, S., 1977. Seismic stratigraphy and global changes of sea level: Part 3. Relative changes of sea level from Coastal Onlap: section 2. Application of seismic reflection Configuration to Stratigraphic Interpretation. In: Payton, C.E. (Ed.), Seismic Stratigraphy—Applications to Hydrocarbon Exploration, vol. 26. AAPG Mem, pp. 53–62.
Wethington, N.W., Pranter, M.J., 2018. Stratigraphic architecture of the Mississippian limestone through integrated electrofacies classification, Hardtner Field area. Kansas and Oklahoma. Interpretation. 6 (4), 95–115. https://doi.org/10.1190/INT-2018-0042.1.
Wignall, P.B., Twitchett, R.J., 1996. Oceanic anoxia and the End Permian mass extinction. Science 272 (5265), 1155–1158. https://doi.org/10.1126/science.272.5265.1155.
Zachos, J., Pagani, M., Sloan, L., Thomas, E., Billups, K., 2001. Trends, rhythms, and aberrations in global climate 65 Ma to present. Science 292 (5517), 686–693.
Zecchin, M., Caffau, M., 2011. Key features of mixed carbonate-siliciclastic shallow-marine systems: the case of the Capo Colonna terrace (southern Italy). Ital. J. Geosci. 130 (3), 370–379.